Energetics Underlying Hemin Extraction from Human Hemoglobin by Staphylococcus aureus

Megan Sjodt^{a-b}, Ramsay Macdonald^{a-b}, Joanna D. Marshall^a, Joseph Clayton^d, John S. Olson^e, Martin Phillips^a, David A. Gell^f, Jeff Wereszczynski^d and Robert T. Clubb^{a-e*}

^aDepartment of Chemistry and Biochemistry, ^bUCLA-DOE Institute of Genomics and Proteomics and ^cMolecular Biology Institute. University of California, Los Angeles, 611 Charles Young Drive East, Los Angeles, CA 90095, USA; ^dDepartment of Physics and Center for Molecular Study of Condensed Soft Matter, Illinois Institute of Technology, Chicago, IL 60616, USA; ^eDepartment of BioSciences, Rice University, Houston, Texas 77251, USA; ^fSchool of Medicine, University of Tasmania, Hobart, Tasmania 7000, Australia.

Running Title: Energetics of hemin extraction from hemoglobin by S. aureus

*To whom correspondence should be addressed: Prof. Robert T. Clubb, Department of Chemistry and Biochemistry, University of California, Los Angeles, 602 Boyer Hall, Los Angeles, CA 90095. Tel.: 310-206-2334; Fax: 310-206-4749; E-mail: rclubb@mbi.ucla.edu.

Keywords: Bacterial pathogenesis, Receptor, Iron regulated surface determinant system, NEAT domain, IsdH, IsdB, Hemoglobin, Stopped-flow spectrophotometry, Isothermal titration calorimetry (ITC), Molecular Dynamics

ABSTRACT

Staphylococcus aureus is a leading cause of lifethreatening infections in the United States. It actively acquires the essential nutrient iron from human hemoglobin (Hb) using the iron-regulated surface-determinant (Isd) system. This process is initiated when the closely related bacterial IsdB and IsdH receptors bind to Hb and extract its hemin through a conserved tri-domain unit that contains two NEAr iron Transporter (NEAT) domains that are connected by a helical linker domain. Previously, we demonstrated that the tridomain unit within IsdH (IsdH^{N2N3}) triggers hemin release by distorting Hb's F-helix. Here, we report that IsdH^{N2N3} promotes hemin release from both the α and β subunits. Using a receptor mutant that only binds to the α-subunit of Hb and a stoppedflow transfer assay, we determined the energetics and micro-rate constants of hemin extraction from tetrameric Hb. We found that at 37°C, the receptor accelerates hemin release from Hb up to 13,400fold, with an activation enthalpy of 19.5 ± 1.1 kcal/mol. We propose that hemin removal requires the rate-limiting hydrolytic cleavage of the axial

HisF8 Ne-Fe³⁺ bond, which, based on molecular dynamics simulations, may be facilitated by receptor-induced bond hydration. Isothermal titration calorimetry experiments revealed that two distinct IsdH^{N2N3}-Hb protein-protein interfaces hemin release. promote A high-affinity receptor:Hb(A-helix) interface contributed ~95% of the total binding standard free energy, enabling much weaker receptor interactions with Hb's Fhelix that distort its hemin pocket and cause unfavorable changes in the binding enthalpy. We present a model indicating that receptorintroduced structural distortions and increased solvation underlie the IsdH-mediated hemin extraction mechanism.

INTRODUCTION

Staphylococcus aureus is an opportunistic Gram-positive pathogen that causes a wide range of illnesses such as pneumonia, meningitis, endocarditis, toxic shock syndrome, bacteremia, and septicemia (1). Methicillin resistant *S. aureus* (MRSA) and other drug resistant strains are a leading cause of life-threatening hospital- and

community-acquired infections in the United States (2, 3). S. aureus requires iron to proliferate, which it actively procures from its human host during infections (4-7). Heme (protoporphyrin IX + iron) present within hemoglobin (Hb) accounts for ~75-80% of the total iron found in the human body and is preferentially used by S. aureus as an iron source (6, 7). Consequently, S. aureus and other microbial pathogens have evolved elaborate heme-acquisition systems to exploit this rich iron source. An understanding of the molecular mechanism of heme scavenging will provide insight into how this pathogen survives and persists within its human host and it could lead to new anti-infective agents that work by limiting microbial access to iron.

S. aureus uses the iron-regulated surface determinant (Isd) system to extract the oxidized form of heme from Hb (hereafter called hemin). The Isd system is comprised of nine proteins that form a hemin relay system that captures Hb and rapidly extracts its hemin, transfers hemin across the cell wall, and then pumps the hemin into the cytoplasm where it is degraded to release free iron (8-10). Four Isd proteins (IsdA, IsdB, IsdC, and IsdH/HarA) are covalently linked to the bacterial cell wall via sortase transpeptidases (11, 12). The two surface receptor proteins, IsdH and IsdB, first bind Hb and extract its hemin (13-17). Then the hemin is passed to IsdA, which is partially buried in the cell wall (18). Holo-IsdA subsequently transfers hemin to the fully buried IsdC protein via an ultra-weak handclasp complex (19-22). Lastly, holo-IsdC delivers the hemin to the bacterial ABC transporter complex, IsdDEF, which pumps hemin into the cytoplasm where it is degraded to release free iron by the hemin oxygenases, IsdG or IsdI (23, 24). The Isd system is important for S. aureus virulence, as strains lacking genes that encode for components of the system display attenuated infectivity in mouse models and are impaired in their ability to utilize hemin or Hb as the sole source of iron (7, 11, 25-27). Related hemin acquisition systems are used by other Grampositive pathogens to obtain iron.

Hemin is extracted from the oxidized form of Hb (called methemoglobin) using the *S. aureus* IsdB and IsdH receptors (15, 16, 28–31). The receptors share similar primary sequences and contain NEAr iron Transporter (NEAT) domains,

binding modules originally named because they were found in bacterial genes that are proximal to putative Fe³⁺ siderophore transporter genes (32). Our previously published studies of IsdH have shown that it extracts hemin using a tridomain unit formed by its second (N2) and third (N3) NEAT domains, which are connected by a helical linker domain (IsdH^{N2N3}, residues A326-D660) (**Fig. 1a**). Studies using native MetHb have shown that IsdH^{N2N3} rapidly extracts hemin from Hb, ~500fold faster than the rate at which hemin spontaneously dissociates from Hb. Recent NMR and crystallography studies of the Hb-free and bound forms of IsdH have provided insight into how it promotes hemin release from Hb (29-31). Crystal structures of the Hb:IsdH^{N2N3} complex reveal that the receptor adopts an extended dumbbell shape structure in which the N2 domain engages the A- and E-helices of Hb, while the N3 domain is positioned within 12 Å of the hemin molecule that is located on the same globin chain (Fig. 1b). Hemin release may in part be triggered by the helical linker domain, which distorts the Fhelix in Hb that houses the iron-coordinating proximal histidine residue (HF8) (Fig. 1c). NMR studies of the apo-receptor uncovered the presence of inter-domain motions between the N2 and linker domains, revealing that the receptor adaptively recognizes Hb. IsdB shares significant primary sequence homology with IsdH and actively acquires hemin from Hb, suggesting that it also employs a semi-flexible tridomain unit to extract Hb's hemin (16, 22, 28, 33).

While the structural basis of IsdH binding to Hb is now understood, we lack a quantitative understanding of the mechanism of hemin transfer. This is because the heterogeneous nature of the transfer reaction, which has thus far limited its detailed biophysical characterization. For example, at the concentrations used to monitor hemin release, Hb adopts distinct tetrameric and dimeric quaternary states that have different propensities to release hemin (34, 35). Moreover, IsdH binds to both the α - and β -globin chains within Hb, which also release hemin at different rates (36, 37). Finally, hemin extraction causes Hb to dissociate into its component globin chains, irreversibly aggregate and release hemin faster than intact Hb (38, 39). Thus, previously measured rates of hemin transfer using wild-type Hb and IsdH report on an amalgamation of distinct extraction processes, hindering a quantitative understanding of the energetics that underlie hemin extraction. To overcome these limitations we used a stabilized tetrameric form of Hb and a bacterial receptor mutant that only binds to Hb's α -subunit. We show using stopped-flow experiments that the tridomain unit accelerates hemin release from the α -subunit by more than 10,000 fold, a rate that is significantly faster than previously reported values that were measured using heterogeneous components. requires a Gibbs activation energy of 18.1 ± 1.1 kcal/mol to be surmounted, whose high enthalpic component suggests that in the transition state the proximal histidine-hemin bond (Ne-Fe) bond is hydrolytically cleaved. Molecular dynamics (MD) simulations suggest that the receptor's ability to lower the activation energy by ~6 kcal/mol is due to its ability to induce strain in the bond and to increase the concentration of nearby water molecules that compete with Hb's HisF8 Ne atom for the iron atom within hemin. Quantitative measurements of Hb-receptor binding interactions using Isothermal titration calorimetry (ITC) indicate that two energetically distinct receptor-Hb interfaces form the pretransfer complex. An interface between the receptor's N2 domain and the A-helix of Hb is the primary contributor to overall binding affinity, tethering IsdH to Hb to enable lower affinity interactions that distort Hb's hemin pocket. A model of the hemin extraction process is presented that incorporates the existing structural, kinetics and thermodynamic binding data.

RESULTS

Development of a quantitative assay to study hemin extraction. We developed an assay to quantitatively measure the kinetics of IsdH-mediated hemin removal from the α-globin chain within tetrameric Hb. In the assay a mutant of IsdH^{N2N3} that only binds to the α-subunit of Hb is used (α-IsdH, residues A326-D660, with 365 FYHYA $^{369} \rightarrow ^{365}$ YYHYF 369 mutations). α-IsdH contains F365Y and A369F mutations within the alpha-helix of the Hb binding N2 domain, which selectively weakens its affinity for the β-subunit in Hb (31). The assay also employs Hb0.1, a tetramer

stabilized recombinant form of Hb in which the two α -subunits are present within a single polypeptide (the C-terminus of one α -subunit is joined via a glycine residue to the N-terminus of the second α -subunit (40)). Hb0.1 also contains a V1M mutation that facilitates expression in *E. coli*, but is otherwise structurally and functionally identical to wild-type Hb. Because Hb0.1 has a significantly reduced propensity to dissociate into $\alpha\beta$ Hb dimers, hemin transfer experiments employing it and α -IsdH enables hemin extraction from the α -globin chain within tetrameric Hb to be selectively monitored (35, 40).

As summarized in Table 1, analytical ultracentrifugation (AUC) sedimentation equilibrium experiments confirm that α-IsdH binds tetrameric Hb0.1 with the appropriate 2:1 stoichiometry via interactions with its α -subunits. In the AUC experiments, to prevent complications caused by hemin transfer, Hb0.1 was maintained in its carbonmonoxy ligated state and heminbinding deficient IsdH proteins were used that contain a Y642A mutation that removes the iron coordinating tyrosine residue (41). In all AUC experiments the concentration of Hb0.1 was monitored by measuring its absorbance at 412 nm, the Soret band of the bound heme molecule. As expected, isolated Hb0.1 forms a stable tetramer at concentrations that are used in hemin transfer experiments; at 5 µM (heme units), Hb0.1 has a weighted average molecular mass of $64,212 \pm 829$ Da at $13,000 \times g$. We next used AUC to determine the Hb0.1:α-IsdH^{Y642A} binding stoichiometry when α -IsdH^{Y642A} is present at a 15-fold molar excess. This data indicates that ~1.8 α -IsdH Y642A proteins bind to each Hb0.1 tetramer, compatible with it only binding to the α -subunits. Increasing the ratio of α -IsdH Y642A to Hb0.1 in the AUC experiments to 30:1 does not increase this stoichiometry, indicating that Hb0.1 is saturated (Fig. 2a, red curve). In contrast, IsdHY642A, which is identical to α -IsdH Y642A except that it does not contain mutations in the Hb contacting alphahelix, binds to Hb0.1 with a stoichiometry of ~3.2 (Fig. 2a, blue). This is consistent with previous studies that have shown that IsdHY642A binds to both the α - and β -subunits of Hb (31, 42). To confirm that α -IsdH Y642A interacts with only the α subunits within Hb0.1, AUC experiments were

performed using the β-CO tetramer, which only contains the isolated β -globin protein (**Fig. 2b**). Consistent with previously reported studies, AUC analysis of the β -CO form indicates that it adopts a tetrameric structure; molecular mass of 56,700 ± 724 Da at $6000 \times g$ (56,300 ± 508 Da at 13,000 × g) (35, 43). When the AUC studies are repeated in the presence of excess IsdHY642A, the receptor binds to the β -CO tetramer with stoichiometry indicating that it can bind to the βglobin chain, but steric effects caused by tetramerization may limit receptor occupancy (molecular mass of 134,000 \pm 1321 Da at 6000 \times g) (Fig. 2b, blue). Interestingly, when similar experiments are performed using α -IsdH^{Y642A}, no detectable binding is observed (Fig. 2b, red). Overall, the results of these studies indicate that the α -IsdH Y642A receptor only binds to the α subunits within Hb0.1 and that both of these subunits are nearly saturated with the receptor at a α -IsdH Y642A :Hb0.1 of 15:1, (Hb0.1 ratio concentration 5 µM heme units). These conditions and reagents were therefore used in subsequent stopped-flow hemin transfer experiments to preferentially measure the rate at which the receptor extracts hemin from the α-subunit of tetrameric Hb0.1.

Hb tetramerization slows hemin removal from Stopped-flow the α-subunit. **UV-Vis** spectroscopy was used to measure the rate at which α-IsdH extracts hemin from either the stabilized Hb0.1 tetramer or native Hb (results summarized in Table 2). In these experiments, the proteins were rapidly mixed, and the amount of hemin transfer was determined by monitoring UV absorbance changes at 405 nm (29, 35). A 30-fold molar excess of receptor was employed (5 and 150 µM of Hb and receptor, respectively) to ensure that α -IsdH saturates the α -globin subunit (Table 1). Upon mixing, a rapid shift in the UV-spectrum occurs indicating hemin transfer from Hb0.1 to α-IsdH (Fig. 3a). The time-dependent spectral changes exhibit biphasic kinetics, with approximately half of the total magnitude of the spectral change characterized by a rapid event defined by the rate constant k_{fast} and the remaining, much slower changes, described by k_{slow} (**Fig. 3b**). Importantly, hemin transfer is completed during

the time course of the experiment, as minimal additional spectral changes are observed when the proteins are incubated overnight. As the receptor is in excess and has higher affinity for hemin than hemoglobin (described below), we conclude that all of the hemin in Hb0.1 is captured by α -IsdH. The observed pseudo-first-order rate constants, k_{fast} and k_{slow} , are 0.34 \pm 0.01 s⁻¹ and 0.026 \pm 0.001 s⁻¹ at 25°C, respectively. As α-IsdH only binds to the α-subunits of the stabilized Hb0.1 tetramer, we conclude that the rapid changes characterized by $k_{\rm fast}$ describe hemin removal from the α -subunit within tetrameric Hb0.1, while the slower changes result from indirect hemin capture from the βsubunit after it has first been released into the solvent. Indirect hemin capture from the β-subunit is consistent with the value of k_{slow} , as it is similar in magnitude to the previously reported rate at which the β -subunit spontaneously releases hemin into solvent from the semihemoglobin form of tetrameric Hb $(0.007-0.013 \text{ s}^{-1})$ (35, 39). Moreover, the value of k_{slow} is independent of receptor concentration (Fig. 5b). The tetrameric α subunit spontaneously releases hemin into the solvent at a rate of ~ 0.000083 s⁻¹ at 37°C. Thus, α -IsdH accelerates the rate of hemin release from the α-subunit ~13,400-fold, and scavenges hemin from the β -subunit indirectly via the solvent.

To investigate the impact of the dimertetramer Hb equilibrium on hemin capture we measured transfer rates to α-IsdH from Hb, which exists as a mixture of dimeric $(\alpha\beta)$ and tetrameric $(\alpha_2\beta_2)$ species that have differing propensities to release hemin (35). Stopped-flow experiments indicate that hemin is rapidly removed from Hb, with k_{fast} and k_{slow} rate constants of 3.27 ± 0.07 s⁻¹ and 0.041 ± 0.001 s⁻¹¹ at 25°C, respectively. As for Hb0.1, k_{fast} accounts for approximately half of the overall spectral change that occurs upon receptor mixing with Hb, consistent with it reporting on the rate of hemin removal from the α-subunit. Interestingly, as compared to Hb0.1, the k_{fast} for hemin removal from Hb is increased ~9-fold (Fig. 3c). This is consistent with the presence of dimeric species in the reaction containing Hb that are known to release hemin more rapidly than the tetrameric Hb, and the fact that upon hemin removal, Hb can fully dissociate into monomeric α-globin chains that have even weaker affinity for

hemin (15, 35). More modest 2-fold increases in k_{slow} are also observed when Hb is used instead of Hb0.1 (**Fig 3d**). They are consistent with the production of isolated β -subunits produced upon Hb dissociation that are known to more rapidly release hemin than tetrameric Hb0.1 (35). However, as this process occurs slowly, α -IsdH presumably extracts hemin from the β -subunits through an indirect process in which the hemin is first released into the solvent

Hemoglobin tetramer dissociation also accelerates the rate of hemin capture by the native IsdH^{N2N3} receptor that binds to both the α - and β -globin chains. This was demonstrated by measuring the rate of hemin transfer to IsdH^{N2N3} from either Hb or the stabilized Hb0.1 tetramer (**Fig. 3b**). With IsdH^{N2N3}, as with α -IsdH, hemin is removed from Hb0.1 more slowly than it is from Hb, consistent with the reduced propensity of Hb0.1 to dissociate into more labile dimeric and monomeric species upon hemin removal (**Fig. 3c**).

monomeric species upon hemin removal (**Fig. 3c**). Therefore, the IsdH N2N3 receptor's faster kinetics of hemin removal from Hb0.1 may be caused by its ability to also remove hemin from hemoglobin's β -subunit, which is known to release hemin more readily than the α -subunit (35). Combined, these data indicate that the propensity of Hb to dissociate during the extraction process increases the overall observed rate of transfer to the receptor by producing partially hemin ligated states (semi-forms) or dissociated forms of hemoglobin that have a greater propensity to release their hemin molecules.

IsdH extracts hemin from both the α- and β-subunits in an effectively irreversible process. The stopped-flow and AUC data indicate that IsdH actively extracts hemin from the α-subunit (Figs. 2-3), but it is not known if the receptor also triggers hemin release from the β-subunit. We therefore probed the ability of IsdH^{N2N3} to remove hemin from tetrameric Metβ, which only contains β-globin chains bound to hemin (Fig. 4). Active removal is observed when IsdH^{N2N3} is added to Metβ, with rapid changes in the absorbance spectrum observed within 5 seconds of mixing. A detailed interpretation of the kinetics data is not possible because the β-globin chains aggregate after hemin is removed. However, extraction from

Metβ occurs at a rate of ~3 s⁻¹, which is similar to the rate at which IsdH^{N2N3} removes hemin from Hb and about 4-times faster than Hb0.1. This is compatible with previous studies that have shown that hemin loss from Metß tetramers is comparable to that of β -subunits within tetrameric Hb (35), and it suggests that IsdH^{N2N3} may remove hemin more rapidly from the β-subunit within Hb than from its α -subunit. In contrast to IsdH^{N2N3}, only modest spectral changes are observed when α -IsdH is added to Metß (Fig. 4). This is compatible with α -IsdH's inability to bind the β -CO tetramer (Fig. 2b), such that it must indirectly scavenge hemin after it has first been released into the solvent. This supported by control transfer studies using recombinant H64Y/V68F apo-myoglobin (apo-Mb containing H64Y and V68F mutations), which does not physically interact with Metß and like α -IsdH slowly scavenges its hemin (**Fig. 4**) (39). Combined, these results indicate that native IsdH N2N3 actively removes hemin from both the α and β -globin chains within human hemoglobin.

To the best of our knowledge, the relative hemin binding affinities of IsdH^{N2N3} and Hb have not been reported. We therefore performed hemin binding competition assays in which each protein was separately mixed with the apo-Mb reagent, which has a known affinity for hemin and whose hemin binding can readily be measured at 600 nm (39). Mixing either 5 µM of Hb or Hb0.1 with a 10-fold molar excess of apo-Mb results in a measurable increase in absorbance at 600 nm indicating that hemin is transferred to apo-Mb (Fig. 5a). As expected, both transfer processes occur slowly, compatible with hemin first being released into the solvent by hemoglobin before it is subsequently bound by the apo-Mb reagent. These data indicate that apo-Mb has significantly higher affinity for hemin than Hb and Hb0.1. This is compatible with previously reported hemin dissociation constants (K_{-H}) of Hb and apo-Mb; the K_{-H} of apo-Mb is ~0.03 pM, whereas K_{-H} for dimeric Hb is 1.7 and 42 pM for its α and β chains, respectively, and the K_{-H} for tetrameric Hb is 0.8 and 4.2 pM for its α and β chains, respectively (35). Notably, the transfer data reveal that Hb0.1 releases hemin more slowly than Hb (Fig. 5a), consistent with previous studies that have shown that the tetrameric form of Hb releases hemin more slowly than the dimeric form (35). In

contrast, when hemin containing IsdH^{N2N3} is mixed with the apo-Mb reagent only small absorbance changes are observed at 600 nm, indicating that unlike Hb and Hb0.1, the receptor has higher affinity for hemin than apo-Mb. Similar to IsdH N2N3 , mixing α -IsdH with apo-Mb results in minimal absorbance changes (data not shown). This is expected as mutations in α -IsdH that confer a-globin binding selectivity are located in the N2 domain and are distal to the hemin binding pocket located in the N3 domain. Taken together, we conclude that IsdH N2N3 and α -IsdH bind hemin with $K_{\rm H}$ values < ~0.03 pM, such that they have substantially higher affinity for hemin than Hb or Hb0.1. Therefore, during the time-frame of the stopped-flow experiments transfer of hemin from hemoglobin to the receptor is effectively unidirectional and irreversible.

Determination of the micro-rate constants describing hemin removal from the α -subunit.

To estimate the micro-rate constants that describe hemin removal, the kinetics data were interpreted using scheme I. In this reaction, hemin-bound Hb0.1 first forms a complex with α -IsdH described by the association and dissociation rate constants, k_1 and k_{-1} , respectively. Within the Hb[hemin]: α -IsdH pretransfer complex, hemin is transferred from the α -subunit of tetrameric Hb0.1 to α -IsdH in a process described by $k_{\rm trans}$. This yields a semi-form of Hb0.1 in which one hemin molecule has been removed and the protein remains bound to α -IsdH.

Hb[hemin] + "IsdH
$$\rightleftharpoons_{k_{-1}}^{k_{1}}$$
 Hb[hemin]:"IsdH $\rightleftharpoons_{trans}^{k_{trans}}$ Hb:"IsdH[hemin]

Scheme I

At the conditions used in our stopped-flow experiments, measured values of $k_{\rm fast}$ describe the kinetics of this entire process and account for the simultaneous removal of hemin from both α -subunits. Contributions to $k_{\rm fast}$ caused by hemin removal from the β -subunit are also possible, but are expected to be minimal as α -IsdH does not bind to this subunit or actively extract its hemin (Fig. 4 and Table 1). To estimate the micro-rate constants, stopped-flow hemin transfer

experiments were performed using varying amounts of α -IsdH in its hemin-free form. At all receptor:Hb0.1 stoichiometries k_{fast} accounted for ~50% of the total spectral change consistent with it monitoring hemin removal from only the αsubunit (Fig. 3b), and the pseudo first order values for k_{fast} increased hyperbolically with increasing receptor concentrations (Fig. 5b, dark grey circles). This is compatible with the rapid formation of a Hb:α-IsdH complex, followed by rate-limiting transfer of hemin to the receptor. In the transfer experiments, [heme-free α -IsdH] is \geq 10[Hb0.1], such that the rate of hemin transfer is pseudo-first-order and the fraction of pre-transfer complex is small and in steady state during the reaction. The dependence of k_{fast} on the micro-rate constants and receptor concentration can therefore be described by Eqn. 1 (44),

$$k_{fast} = \frac{k_1 k_{trans} [\alpha - IsdH]}{k_1 [\alpha - IsdH] + k_{-1} + k_{trans}}$$
(Eqn. 1)

where k_1 , k_{-1} , and k_{trans} are the micro-rate constants of the individual reaction steps. As shown in Fig. 5b, fitting of the kinetics data using Eqn. 1, yields values of $2.8 \times 10^7 \text{ M}^{-1} \cdot \text{s}^{-1}$, $2.4 \times 10^3 \text{ s}^{-1}$, and $0.57 \pm$ 0.02 s^{-1} for k_1 , k_{-1} , and k_{trans} , respectively. The fitted value of k_{-1} is much larger than k_{trans} , and as result, only the ratio k_{-1}/k_1 and not the absolute values of these constants are well defined by the observed data. The equilibrium dissociation constant (K_D) for the Hb0.1:α-IsdH pretransfer complex calculated from the micro-rate constants is 85.7 \pm 3.8 μ M (k₋₁/k₁ = K_D), a value that is consistent with dissociation constants measured using ITC (described below). The k_{slow} values do not depend on the concentration of the receptor, consistent with it describing absorbance changes caused by hemin release into the solvent from the β-globin chain followed by uptake by α -IsdH (**Fig. 5b**, light grey circles).

An enthalpic barrier must be surmounted to capture hemin. Stopped-flow experiments were performed at temperatures ranging from 15 to 37°C using a molar ratio of 1:40 Hb0.1: α -IsdH (**Fig. 6a**). At this Hb:receptor ratio the contribution of k_{-1}/k_I to $k_{\rm fast}$ becomes negligible, such that $k_{\rm fast} \approx k_{\rm trans}$ (44). A plot of $\ln(k_{\rm trans}/T)$

versus 1/T enables the activation parameters to be determined using the linearized form of the Eyring equation,

$$ln\frac{k}{T} = ln\left(\frac{k_B}{h}\right) + \frac{\Delta S^{\ddagger}}{R} - \frac{\Delta H^{\ddagger}}{RT}$$
 (Eqn. 2)

where $k_{\rm B}$, h, and R are the Boltzmann, Planck, and ideal gas constants, respectively. The activation enthalpy (ΔH^{\ddagger}) and entropy (ΔS^{\ddagger}) are calculated from slope and intercept, respectively (Fig. 6b). This analysis yielded ΔH^{\ddagger} and ΔS^{\ddagger} values of 19.45 \pm 1.1 kcal/mol and 4.45 \pm 0.31 cal/mol·K, respectively, and a ΔG^{\ddagger} value of 18.07 \pm 1.1 kcal/mol at 37°C. Previous studies have shown that hemin dissociates from the α-globin chain of tetrameric Hb at a rate of 0.000083 s⁻¹ (35), which based on the Arrhenius equation indicates that the ΔG^{\ddagger} for spontaneous hemin release is 23.96 kcal/mol at 37°C. Thus, the receptor lowers the activation energy needed to release hemin from the α -subunit by ~5.9 kcal/mol, accelerating the rate ~10,000-fold (k_{trans} = 0.88 s⁻¹ vs. 0.000083 s⁻¹ at 37°C).

Two energetically distinct receptor-Hb interfaces are used to bind Hb and distort its hemin pocket. The crystal structure of the Hb:IsdH^{N2N3} complex reveals that the receptor alters the structure of the hemin binding pocket within Hb, presumably weakening its affinity for hemin (31). Two receptor-Hb interfaces are present in the structure, the N2 domain binds to Hb's A-helix, while the linker and N3 domains contact the F-helix within the same globin (Fig. 1b). These contact surfaces are extensive, burying 618 and 688 A² of surface area, respectively. Previously, we have shown that polypeptides containing only the N2 (IsdH^{N2}) and linker-N3 (IsdH^{LN3}) domains of the receptor autonomously folded, and that IsdH^{LN3} forms a rigid structure (15, 29). Using these protein constructs ITC experiments were performed to gain insight into how each interface contributes to the energetics of Hb binding (Table 3). Initially, binding of α-IsdH^{Y642A} to the carbonmonoxy form of Hb (HbCO) was investigated. As expected, no heme transfer occurs between these proteins when monitored by UV-vis spectroscopy (not shown) enabling the protein binding energetics to be

quantified. In the ITC experiments, a syringe filled $\mu M \quad \alpha\text{-IsdH}^{Y642A}$ was 200 injected incrementally into a cell containing 30 µM of HbCO, and the ensuing heat changes were used to generate a binding isotherm (Fig. 7a). Consistent with the AUC data, α-IsdH^{Y642A} binds Hb at a ratio of ~2:1 (Tables 1 and 3). The measured K_D value for complex is $4.0 \pm 0.6 \mu M$ and is of similar magnitude as the value obtained from an analysis of the kinetics data. At 25°C, the standard enthalpy (ΔH^{o}) and entropy (ΔS^{o}) of receptor binding are - 6.0 ± 0.5 kcal/mol and 4.6 ± 1.9 cal/mol·deg, respectively (ΔG° -7.4 ± 0.1 kcal/mol). To selectively probe binding by the N2 domain, a polypeptide containing only the N2 domain of α-IsdH with the appropriate amino acid mutations that confer binding selectivity for the α -globin chain was studied (α-IsdH^{N2}, residues A326-P466 of α -IsdH). ITC measurements indicate that α -IsdH^{N2} binds HbCO with a K_D of 7.5 \pm 1.1 μ M and similar ~2:1 stoichiometry (Fig. 7b). Interestingly, the entropy change associated with HbCO binding is unfavorable for α -IsdH^{N2} (Δ S° = -11.1 ± 2.0 kcal/mol·deg), but favorable for intact α-IsdHY642A. This difference likely arises from unfavorable ordering of the alpha-helix within the N2 domain that accompanies Hb binding (30, 45), which, in the context of the longer α-IsdH^{Y642A} protein, are masked by other entropic changes caused by interactions originating from the linker and N3 domains (29, 45).

ITC binding studies were also performed using a polypeptide that contains only the linker and N3 domains of IsdH (IsdH^{LN3}, residues P466-D660, containing a Y642A mutation in the N3 domain to prevent hemin binding). IsdH^{LN3} binds to HbCO, but these interactions are too weak to be accurately quantified. Nevertheless, it is evident from the ITC data that HbCO binding by IsdH^{LN3} is endothermic (Fig. 7c), consistent with the crystal structure of the complex that revealed that this portion of the receptor partially unwinds Hb's F-helix. NMR spectroscopy experiments confirm that IsdH^{LN3} and HbCO interact weakly, as crosspeaks in the ¹H-¹⁵N HSQC spectrum of ¹⁵Nenriched IsdH^{LN3} are attenuated and broadened only when large amounts of unlabeled HbCO are added (Fig. 7d, right). The binding affinity is very weak, with an estimated K_D in the mM range.

Weak HbCO-IsdH^{LN3} interactions require both the linker and N3 domains in IsdH^{LN3}, as no interactions are observed when HbCO is added to a ¹⁵N-enriched IsdH^{N3} polypeptide that only contains the N3 domain (**Fig. 7d**, left). Thus, IsdH uses two energetically distinct interfaces to bind Hb. A high affinity interface formed between the IsdH N2 domain and Hb's A-helix tethers the receptor to Hb, enabling a second, much weaker interface to form in which the F-helix is distorted.

Molecular dynamics simulations reveal the receptor promotes hemin solvation. Hemin release from Hb presumably involves the competitive displacement of the axial histidine NE atom with a water molecule, enabling formation of a new water-Fe³⁺ bond. The observed rate enhancements may therefore in part be due to distortion and increased solvation of the histidine-Fe³⁺ linkage upon receptor binding. To investigate solvation effects of IsdH binding, two explicitsolvent 200ns molecular dynamics (MD) simulations were performed on hemin containing methemoglobin systems: one with, and one without IsdH^{N2N3} bound to the α subunit (**Fig. 8**). Over the course of the simulations, the overall complex structures did not exhibit any large-scale structural rearrangements, and the F-helix in the IsdH^{N2N3} bound structure remained distorted (data not shown). Two analyses were performed to assess the effects of receptor binding on hemin solvation. First, the radial distribution functions (RDFs) of the water hydrogen and oxygen atoms were computed relative to the midpoints of the histidine-iron bonds (Fig. 8b). The RDF plots were normalized such that a value of 1.0 is equivalent to bulk solvent. It was observed that in both systems water molecules were allowed to approach this bond, however, in the IsdHN2N3 bound system, the waters were more frequently observed at locations close to the bond. For example, in the IsdH^{N2N3} bound system water hydrogens were ~17 times more likely to be located within a distance of 2.1 Å, with the integral of the RDF from 0 to 2.1 Å being 0.016 and 0.001 for the bound and free system respectively, and hydrogens were ~2 times more likely to be located within 2.5 Å of the bond center.

To further investigate the location and stability of solvent molecules surrounding the iron-nitrogen bond, we performed a grid inhomogeneous solvation theory (GIST) analysis of our simulations in the region surrounding the receptor bound hemin. This analysis computes the density, energies, and entropies of water molecules in a three-dimensional grid for the specified region over the equilibrated portion of a simulation. We defined a "hydration site" as a position in space in which the occupancies of water oxygen molecules were at least three times greater than water in bulk, and which the estimated free energies of water molecules were less than zero relative to bulk. This definition effectively chooses locations where it is favorable for a water molecule to occupy relative to being in the bulk, which is accounted for by both a thermodynamic analysis, as well as an observed high occupancy. Results of this analysis show that in both the IsdH^{N2N3} free and bound forms of Hb, hydration sites exist within the heme binding pocket. However, when IsdHN2N3 binds to Hb more of these hydration sites occur near the axial His87 residue in Hb (compare Figs. 8c and 8e). Combined with the RDF analysis, these data indicate that the hemin pocket in Hb is never completely devoid of water molecules, and show that when IsdH binds to Hb, closer and more stable hydration occurs near atoms that are proximal to the iron-nitrogen covalent bond. We conclude that receptor introduced distortions in the axial bond that weaken its affinity combined with solvation, favors water competitive displacement equilibrium.

DISCUSSION

S. aureus acquires iron from human hemoglobin using two related surface receptors, IsdH and IsdB (46). The receptors extract Hb's hemin using a conserved tridomain unit that is formed by two NEAT domains that are separated by a helix linker domain (**Fig. 1a**) (15). The mechanism of extraction is best understood for IsdH. Previously, we've shown that the NEAT domains within its tridomain unit (IsdH^{N2N3}) synergistically extract hemin from Hb at a rate that is significantly faster than the rate at which Hb spontaneously releases hemin into the solvent. A 4.2 Å resolution crystal structure of the Hb:IsdH^{N2N3} complex revealed that each receptor engages a single globin chain, with

the N2 domain contacting the globin's A-helix and the N3 domain positioned near its hemin molecule (30). The hemin needs to slide only ~12 Å from the globin into the receptor's N3 domain where its iron atom is coordinated by a tyrosine residue. A subsequent higher resolution 2.55 Å structure of the complex contained the receptor bound to the α globin and revealed it may trigger hemin release by distorting the F-helix that contains the axial histidine residue (HisF8) (31). While atomic structures have provided great insight into the process of hemin extraction, the energetics underling this process are poorly understood. This is because the native IsdH-Hb system is heterogeneous, as Hb exists in dimeric and tetrameric forms that have different propensities to release hemin, and once hemin is removed from Hb it dissociates into its component globins that aggregate and more rapidly release hemin. Furthermore, our stopped-flow results indicate IsdH^{N2N3} extracts hemin from both the α - and β subunits within Hb (Figs. 3 and 4) and that the native IsdH binds to tetrameric Hb with subsaturating stoichiometry (Table 1). Thus, the heterogeneous properties of the native system limit its detailed biophysical characterization.

In order to quantitatively analyze hemin extraction from Hb we developed an assay that preferentially monitors hemin transfer from only its α-subunit. This was accomplished by using a stabilized tetramer of Hb (Hb0.1) and a variant of IsdH N2N3 (α -IsdH) that we show only binds to the α-subunit (**Table 1**). Stopped-flow UV-Vis experiments reveal that α-IsdH captures hemin in a biphasic manner; a rapid phase characterized by k_{fast} describes the active extraction of hemin from the α-globin subunit, while slower spectral changes defined by k_{slow} report on the indirect capture of hemin from the β-subunits after it has first been released into the solvent. The latter conclusion is supported by our finding that the are independent of values $k_{\rm slow}$ concentration (Fig. 5b).

It is possible that some rapid, activated hemin transfer occurs from β -subunits and contributes to the fast phase in the IsdH experiments because our spectral and kinetic measurements do not distinguish between these subunits. The notion of accelerated heme

dissociation from Hb \(\beta\)-subunits is suggested by the results of AUC and hemin transfer experiments both of which indicate that IsdHN2N3 binds to isolated metß subunits and rapidly acquires its hemin. However, the amplitude of the fast phase is 50% in the transfer experiments with both α -IsdH, where only α chains interact with the receptor, and IsdH N2N3 , where some binding to β subunits does occur. This result implies that the fast phase represents activated heme transfer from α subunits in both cases. However, it is conceivable that hemin release from the β-subunit also contributes passively to k_{fast} , as our spectral and kinetic measurements can't distinguish easily between these subunits. Additional experiments using valence hybrid mutants of Hb are required to fully resolve this issue (39).

Our results suggest that the receptor removes hemin at a faster rate from dimeric MetHb (αβ) than it does from tetrameric MetHb $(\alpha_2\beta_2)$, as α -IsdH removes hemin 10-fold faster from native Hb than it does from Hb0.1 (k_{fast} 0.34 and 3.27 s⁻¹, respectively) (**Table 2** and **Fig. 3c**). This conclusion is supported by our AUC data that indicate that Hb0.1 adopts a tetrameric state at the concentrations used in our stopped-flow studies (Table 1), whereas Hb is a mixture of dimeric and tetrameric forms; at the 5 µM hemoglobin concentrations used in this study, ~65% of Hb is tetrameric and ~35% dimeric ($K_{4,2}$ of 1.5 μ M) (35). The larger k_{fast} for native Hb is presumably caused by hemin removal from its dimeric form, which is known to release hemin more rapidly than the tetramer (35). ESI-MS studies have also shown that hemin removal by the receptor causes native Hb to dissociate into its monomeric globin chains (15). This latter process further explains why α-IsdH removes hemin more rapidly from Hb than from Hb0.1, as the isolated globins caused by native Hb dissolution release hemin at faster rates than Hb dimers and tetramers (35). Similar effects are observed for IsdH^{N2N3}, which like α -IsdH, removes hemin more rapidly from native Hb than it does from the stabilized Hb0.1 tetramer. Interestingly, when the k_{fast} values for hemin removal from Hb0.1 are compared, IsdHN2N3 removes hemin ~2-fold faster than α -IsdH (Fig. 3c). We speculate that this difference is caused by the IsdH^{N2N3} receptor's unique ability to also

extract hemin from the β-subunit of Hb0.1, which has weaker affinity for hemin than the α -subunit. This notion is substantiated by the results of AUC and hemin transfer experiments that indicate that IsdH^{N2N3} binds to Metβ and rapidly acquires its hemin. The measured k_{fast} for hemin transfer from Hb0.1 to IsdH^{N2N3} is therefore likely an amalgam of the rates of hemin removal from both types of globin chains within hemoglobin, whereas the k_{fast} of transfer to α-IsdH only reflects hemin removal from the α -globin that binds hemin more tightly. No differences in k_{fast} are observed between the receptors when Hb is employed as the hemin donor, as tetramer dissociation accelerates hemin release thereby masking subtle globin-specific contributions to k_{fast} (Fig. **3b**). complications highlight the benefits of using Hb0.1 and α-IsdH to selectively monitor hemin removal, as the native receptor captures hemin from both globins in a process that is facilitated by Hb dissociation into its component monomeric globins and dimeric Hb (**Table 2**).

The micro-rate constants and energetics of hemin extraction were estimated using data from the α-specific transfer assay. Extraction can be envisioned as occurring through scheme 1, with the ratio of k₋₁/k₁ describing the equilibrium dissociation constant for formation of the Hb:α-IsdH complex, and k_{trans} representing the process that moves hemin from Hb into the receptor. is essentially unidirectional, Transfer competition studies with apoMb indicate that IsdHN2N3 binds hemin with significantly higher affinity than Hb (Fig. 5a). Fitting of this data yielded values of $85.7 \pm 3.8 \, \mu M$ and $0.57 \pm 0.02 \, s^{-1}$ for k_{-1}/k_1 , and k_{trans} , respectively (Fig. 5). The value of k_{trans} is ~60% larger than the measured value of k_{fast} , presumably because Hb is only partially saturated with the receptor at the protein concentrations used in the transfer assay. An Eyring plot of the temperature dependence of k_{trans} reveals that hemin transfer is limited by an enthalpic barrier at 37°C, with $\Delta G^{\ddagger} = 18.1 \pm 1.1$ kcal/mol, and ΔH^{\ddagger} and ΔS^{\ddagger} values of 19.5 \pm 1.1 kcal/mol and $\Delta S^{\ddagger} = 4.5 \pm 0.3$ cal/mol·K, respectively. The activation energy required for spontaneous hemin release from the α -subunit of tetrameric Hb is ~24 kcal/mol (47). Thus, α-IsdH effectively lowers ΔG[‡] by ~6 kcal/mol, consistent

with the ~10,000-fold rate enhancement observed in our hemin transfer experiments as compared to the rate of spontaneous hemin release from Hb.

We hypothesize that breakage of the HisF8-iron is rate limiting in the hemin transfer reaction, and that it occurs through a displacement mechanism in which a water molecule outcompetes HisF8 as a ligand for the Fe(III) atom within hemin (48). The Hb:IsdH^{N2N3} crystal structure may resemble the pretransfer complex (scheme 1), since the hemin in this structure remains bound to Hb via a HisF8-iron bond. After bond breakage, the mostly non-polar hemin would then travel ~12 Å through a predominantly hydrophobic pathway to the receptor's N3 domain to form the post-transfer complex (scheme 1) (31). In the Hb:IsdH^{N2N3} crystal structure the receptor unwinds the F-helix, which may lower the energy required to break the axial bond breakage by inducing strain. Receptor induced distortions could also lower the activation energy by increasing the concentration of water molecules near the bond, increasing the probability that they can outcompete HisF8's Ne atom for hemin's iron atom. Indeed, our MD simulations reveal that receptor binding to Hb causes more stable and closer hydration to occur near the axial bond, perhaps favoring water in the competitive displacement equilibria (Fig. 8). Similar hydration of the space near the Fe-HisF8 bond was clearly observed in the crystal structure of the Leu89(F8)Gly mutant of Mb, which showed a similar 3,000-fold increase in the rate of hemin dissociation at pH 7 (48)

The MD simulations also suggest that the receptor alters the positioning of the HisF8-iron bond, but its quantitative impact on axial bond strength will require the application of more sophisticated computational methods. Interestingly, altering the conformation of the Fhelix may be a general strategy used to modulate Hb's hemin affinity, as helical fluctuations in globin chains have been shown to govern overall affinity (38, 49-53). Moreover, this strategy is employed by the α -Hb stabilizing protein (AHSP), which promotes autooxidation of α -globin chains by binding to a distal site that causes localized distortions in the F-helix (54–56).

Receptor-hemoglobin binding measurements employing ITC reveal that IsdH^{N2N3}

uses two energetically distinct binding interfaces with Hb to form the pretransfer complex (Table 3). The first interface is comprised of the N2 domain that binds to the A- and E-helices of Hb (N2-Hb interface), while the second interface contains the linker and N3 domains that interact with F-helix, EF- and FG-corners of Hb (LN3-Hb interface) (Fig. 1b). Using receptor truncation mutants we demonstrated that the N2-Hb interface drives formation of the pretransfer complex. This is evident from our finding that the IsdH^{N2} polypeptide binds to Hb with similar affinity as the intact tridomain receptor IsdH^{N2N3}, $K_D = 7.5 \pm 1.1$ and $4.0 \pm 0.6 \, \mu M$, respectively (Table 3). Conversely, the LN3-Hb interface that that contains the distorted F-helix forms with very weak affinity as judged by ITC and NMR (K_D > 1 mM). ITC data indicate that unwinding Hb's Fhelix is enthalpically unfavorable, as IsdH^{LN3} binding to Hb causes heat to be absorbed (Fig. 7), a comparison of the binding data for α-IsdH and α-IsdH^{N2} reveals less favorable ΔH° changes occur for the intact α -IsdH receptor as compared to α - $IsdH^{N2} (\Delta H^{o} = -6.0 \pm 0.5 \text{ and } -10.3 \pm 0.5 \text{ kcal/mol})$ for α -IsdH and α -IsdH^{N2}, respectively) (**Table 3**). In contrast, formation of the higher affinity N2-Hb interface causes favorable enthalpic changes and unfavorable changes in binding entropy ($\Delta S^{o} = 11.0 \pm 2$ cal/mol-K). The latter effect is likely caused by ordering of loop 2, which undergoes a disordered-to-ordered transition upon binding Hb's A helix (30, 42, 45). Thus, despite burying similar solvent exposed surface areas, the N2-Hb interface is the primary determinant for overall binding affinity, whereas the LN3-Hb interface forms with very weak affinity because of the large enthalpic penalty that must be paid to distort Hb's F-helix. Recently, binding of IsdH to the Hb-Hp complex was studied by surface plasmon resonance (SPR) and it was reported that native IsdH^{N2N3} binds Hb-Hp with a $K_D \sim 120$ nM (57), which is an order of magnitude higher in affinity than our ITC measured affinity of the Hb-IsdH^{N2N3} complex. This difference may result from the distinct methods that were employed. However, it is interesting to note that both the IsdH^{N1} domain and IsdB have been reported to bind the Hb-Hp complex with higher affinity than Hb alone (58). As these receptors do not contact Hp directly, it is possible that subtle Hp-induced changes in the structure of Hb may increase its binding affinity for IsdH and IsdB. However, remarkably Hp binding prevents hemin transfer from Hb to IsdB in the ternary complex (57). Thus, the Hp induced conformational changes prevent hemin dissociation with and without bound receptor (59).

Our measured binding energetics for α -IsdH are generally similar to those previously reported for IsdB^{N1N2}, which is the analogous tridomain unit within IsdB (33). Nevertheless, there are clear differences. Most notably, IsdB^{N1N2} was reported to bind HbCO with 10-fold higher affinity than IsdH^{N2N3}, and unlike IsdH^{N2} that binds Hb with high affinity, the analogous isolated domain from IsdB (IsdB^{N1}) binds HbCO with weak affinity. Thus, despite a high degree of sequence homology shared by the two receptors, there may be significant biochemical differences whose molecular basis needs to be deciphered.

Our studies enable a free energy reaction coordinate diagram to be constructed that describes the process of receptor-mediated hemin extraction from the α -subunit of Hb (Fig. 9). Prior to engaging Hb, the IsdH^{N2N3} receptor undergoes interdomain motions in which the position of the N2 domain moves with respect to the linker and N3 domains that form a rigid unit (29). In step #1, the higher affinity N2-Hb interface forms ($\Delta G^{o} = 7.0 \pm 0.1$ kcal/mol), contributing ~95% of the total binding standard free energy for the receptor-Hb complex. In step #2, the much weaker Hb-LN3 interface forms, unravelling the F-helix to form the pretransfer complex in a process that is enthalpically unfavorable. It is unclear if Hb binding quenches N2-LN3 inter-domain motions within the receptor. In principle, the two distinct receptor-Hb binding interfaces could form in a concerted manner, with binding at the higher affinity N2-Hb interface nucleating new receptor inter-domain and Hb-receptor interactions that immobilize the receptor on Hb and drive formation of the lower affinity Hb-LN3 interface. However, in the crystal structure of the Hb-IsdH^{N2N3} complex no significant N2-Linker interdomain interactions are observed and electron density for residues Asn465-Glu472 connecting these domains is poorly resolved. Thus, it is possible that inter-domain motions at the N2-Hb interface persist after Hb-IsdH^{N2N3} complex formation, with the N2-Hb interface holding the

mobile LN3 unit near Hb's hemin to increase its effective molarity and the likelihood of forming weak contacts to Hb in which the F-helix is unwound (60). Persistent receptor inter-domain motions within the Hb-IsdH^{N2N3} complex may also facilitate downstream hemin transfer from IsdH to IsdA, since in principle, they would not be reliant upon the complete dissociation of the complex. In step #3, Hb's hemin molecule is transferred to IsdH following 12 Å path that is exposed to the solvent. Transfer requires a Gibbs activation energy of 18.1 ± 1.1 kcal/mol to be surmounted. We hypothesize that this energy is needed to hydrolytically cleave the proximal histidine-hemin bond (Ne-Fe) bond, as ΔH^{\ddagger} is 19.5 \pm 1.1 kcal/mol. The structure of the complex and our MD simulations suggest that the receptor lowers the activation energy by ~6 kcal/mol by inducing strain in the bond and by increasing the concentration of nearby water molecules that compete with HisF8's NE atom for the iron atom within hemin. Based on studies of spontaneous hemin release from Mb and Hb, bond breakage may be facilitated by formation of a hemichrome (61). Indeed, a bis-His hemin complex has recently been observed in the structure of the IsdB-Hb complex (62). The receptor likely extracts hemin from the β-subunit using a similar mechanism, but the energetics of this process remain ill-defined. Once hemin is transferred, the hemin-bound receptor dissociates from Hb, presumably through the two-step process in which the weaker Hb-LN3 interface disengages first (step #4), followed by dissociation of the stronger Hb-N2 interface (step #5). The structure of the posthemin transfer complex is not known, so it is possible that hemin transfer to the N3 domain alters its structure further weakening the Hb-LN3 interface. Transfer is effectively unidirectional as IsdH binds hemin with significantly higher affinity than Hb based on competition studies with apo-Mb.

Hemin removal by the native receptor from wild-type Hb is expected to be significantly more complex and could involve simultaneous removal from both the α - and β -subunits, as well as receptor-induced dissociation of Hb into dimeric and monomeric species. Based on unfolding studies with purified Hbs, receptor mediated hemin removal from wild-type Hb could

cause the formation of a dimeric molten globular intermediate in which the $\alpha 1\beta 1$ interface remains intact, but the heme pocket has partially melted, facilitating the hemin removal from both subunits (63). However, in our structure of the complex only the α F-helix has unfolded. Although we now have an idea about the mechanism and energies that underlie hemin transfer from the α -subunit, it remains unknown how hemin moves between the proteins, how interdomain motions affect this process, and whether there are true mechanistic differences between IsdH and IsdB. The new assay we describe in this paper could be a valuable tool to help answer these questions.

Experimental Procedures

Cloning and protein preparation. IsdH proteins were expressed from pET-28b-based plasmids and initially contained a removable N-terminal hexahistidine-small-ubiquitin-like modifier (SUMO) tag facilitate purification (pHis-SUMO) (64, 65). Protein expressing plasmids, include: pRM208 encoding A326-D660 in IsdH (IsdH^{N2N3}), pRM216 encoding A326-D660 that contains a Y642A substitution (IsdH^{N2N3}-Y642A), pMMS322 encoding A326-D660 with substitution of FYHYA $(365-369) \rightarrow YYHYF (365-369)$ that confers selectivity for the α-globin chain of Hb (α-IsdH^{N2N3}) and pMMS323 containing the same substitution of FYHYA (365-369) → YYHYF (365-369) as wellas a Y642A substitution (α -IsdH^{N2N3}-Y642A) (15, 31, 66). In addition, the pET-28b-based plasmid pSUMO-Mb constructed that expresses recombinant sperm whale myoglobin H64Y/V68F with a removable SUMO tag (Mb^{H64Y/V68F}). The expression plasmids were constructed using standard approaches and made use of the QuickChange site-directed mutagenesis kit, (Stratagene, La Jolla, CA). The proteins were expressed by transforming the aforementioned plasmids into E. coli BL21-DE3 cells (New England Biolabs, Beverly, MA). Protein expression and purification procedures have been described previously (15). Briefly, expression proceeded overnight at 25°C by adding 1 mM isopropyl-β-D-thiogalactoside (IPTG) to cell cultures. The bacterial cells were then harvested by centrifugation, lysed by sonication, and the protein purified using a Co²⁺-chelating column (Thermo Scientific, Waltham, MA). The amino terminal 6x-His-SUMO tag was then cleaved using the ULP1 protease and mixture reapplied to the Co²⁺-chelating column to remove the protease and cleaved SUMO tag. The heminfree forms for the IsdH and Mb proteins were generated by hemin extraction with methyl ethyl ketone followed by buffer exchange into 20 mM NaH₂PO₄, 150 mM NaCl, pH 7.5 (67). Hemin saturated proteins were produced by adding a 1.5 molar excess of hemin to purified protein solutions followed by removal of excess hemin using a Sephadex G-25 column (GE Healthcare) equilibrated with 20 mM Tris-HCl, pH 8.0. Protein-hemin stoichiometries were determined using UV-visible spectroscopy and calculating the A_{Soret}/A_{280} .

Human hemoglobin (Hb) was prepared as previously described from the blood of a healthy donor provided by the CFAR Virology Core Lab at the UCLA AIDS Institute (68). Briefly, red blood cells were washed in 0.9% NaCl solution and then lysed under hypotonic conditions. Hb was purified from the hemolysate by two ionexchange chromatography steps, cation-exchange (SP Sepharose, GE Healthcare Life Sciences) followed by anion-exchange chromatography (Q Sepharose, GE Healthcare Life Sciences). During the purification, the globin chains were maintained in the carbon monoxide-liganded state to inhibit autooxidation and subsequent denaturation. genetically stabilized Recombinant human expressed hemoglobin was from plasmid pSGE1.1-E4 in E. coli BL21-DE3 cells, and contains V1M mutations in both α- and β-globin chains and a glycine linker between the Cterminus of one α-subunit and the N-terminus of another α-subunit (called Hb0.1) (40, 69). Cells were grown in M9 minimal media containing 3 g/L glucose and 1 g/L NH₄Cl as the sole source of carbon and nitrogen, respectively. Prior to induction, exogenous hemin was added to the cell cultures to a final concentration of 8 µM. Expression was performed at 16°C overnight by adding IPTG to cell cultures to achieve a final concentration of 1 mM. Cells were then harvested by centrifugation, and washed with lysis buffer (50 mM Tris-HCl, 17 mM NaCl, pH 8.5) twice to remove excess hemin. The cell suspension was then purged with a steady stream of CO for 15 min in an ice-water bath. All buffers used during the

purification were kept at pH 8.5 and were purged with CO to prevent heme oxidation. The cells containing recombinant Hb0.1 were lysed by sonication and purified in a single step using a Co²⁺-chelating column (Thermo Scientific. Waltham, MA) via interactions with the naturally occurring His residues on the surface of Hb0.1. The column was washed using three buffers prior to elution with imidazole: 5 column volumes (CV) of lysis buffer (vida supra), 5 CVs wash buffer #1 (20 mM Tris-HCl, 500 mM NaCl, pH 8.5), and 5 CVs wash buffer #2 (20 mM Tris-HCl, pH 8.5). Column-bound Hb was then eluted with 5 CVs of elution buffer (20 mM Tris-HCl, 100 mM imidazole, pH 8.5).

Hemin transfer experiments. Ferric Hb and Hb0.1 (methemoglobin) were used in the hemin transfer experiments. They were produced by converting the carbonmonoxy-form of each pure protein into the ferric form using established methods and described for Hb. Briefly, HbCO was converted into HbO₂ by delivering a pure stream of oxygen gas over HbCO solution kept cold in an ice-water bath and simultaneously illuminated with a highintensity (100 W) light source. Removal of CO from HbCO and conversion to HbO2 was considered complete when the ratio of A₅₇₇:A₅₆₀ was ~1.8 (70). Oxidation of HbO₂ to generate ferric Hb was achieved by incubating HbO2 with a five-fold molar excess of potassium ferricyanide followed by application of the sample to a Sephadex G-25 column (GE Healthcare) to remove the excess ferricyanide. Ferric Hb (or Hb0.1) was then buffer exchanged into 20 mM NaH₂PO₄, 150 mM NaCl, pH 7.5. The concentration of hemin within each form of the protein was determined using the extinction coefficient of 179 mM⁻¹ cm⁻¹ at a wavelength of 405 nm (71).

The kinetics of hemin transfer from ferric Hb (donor) to apo-IsdH proteins (acceptor) were measured using an Applied Photophysics SX18.MV stopped-flow spectrophotometer (Applied Photopysics, Surrey, UK). Acceptor and donor proteins were dissolved in 20 mM NaH₂PO₄, 150 mM NaCl, pH 7.5 supplemented with 0.45 M sucrose to prevent absorbance changes caused by apoprotein aggregation (39). Ferric Hb was mixed with apo-acceptor present at

≥ 10 molar excess (in hemin units) in order to maintain pseudo-first-order conditions. After rapid mixing (dead-time 3 ms) absorbance changes at 405 nm were monitored for 1000 s. Experiments were performed in triplicate and the data analyzed by fitting the observed time courses to a doublephase exponential expression using the GraphPad Prism program (GraphPad Software, version 5.01). As described in the text, micro-rate constants describing the hemin transfer were obtained by fitting the dependence of the observed fast phase kinetic rate constant (k_{fast}) on the concentration of apo-receptor (Eq. 1) using Mathematica software (Wolfram Mathematica 9.0, Wolfram Research). For slower transfer reactions involving apo- ${\rm Mb}^{\rm H64Y/V68F}$ (39) a 10-fold molar excess of apo- ${\rm Mb}^{\rm H64Y/V68F}$ was used and absorbance changes were measured using a conventional UV-vis spectrophotometer. For these reactions the entire UV-Vis spectrum was recorded over 17 h period.

Analytical Ultracentrifugation (AUC). Sedimentation equilibrium runs were performed at 25 °C in a Beckman Optima XL-A analytical ultracentrifuge using absorption optics at 412 nm such that only the heme molecule was detected. The protein concentrations in samples analyzed by AUC were the same as those used for the stoppedflow hemin transfer experiments (20 mM sodium phosphate, 150 mM NaCl, 0.45 M sucrose, pH 7.5). In order to limit hemin transfer during the AUC experiment, IsdH proteins contained Y642A mutation that limits heme binding and the carbon monoxide-liganded form of Hb0.1 (or β-Hb) was used to limit heme release. Three mm pathlength double sector cells were used for all samples and were purged with CO before sealing the cells to prevent oxidation. Sedimentation equilibrium profiles were measured at speeds of 9,000 (~6,000 \times g) and 13,000 rpm (~13,000 \times g). Samples contained Hb0.1 or β-Hb (isolated β-globin chains) at a concentration of 5 µM and 0, 75 µM, and 150 μM α -IsdH^{Y642A}. Experiments using native IsdH^{Y642A} made use of a 150 μ M sample. Weight-average molecular masses were determined by fitting with a non-linear leastsquares exponential fit for a single ideal species using the Beckman Origin- based software (version 3.01). Partial specific volumes were calculated from the amino acid compositions and corrected to 25°C (72, 73). They were 0.749 for the $\alpha\beta$ Hb heterodimer and β -globin chains, 0.735 for apo-receptor, and 0.739 for the complex. At higher concentrations of receptor, the fitted molecular weights were slightly lower than those obtained when lower receptor concentrations were used, which is compatible with the increased non-ideality of the solution.

Isothermal Titration Calorimetry (ITC). ITC measurements were performed using a MicroCal iTC200 calorimeter (GE Healthcare) at 25°C. To prevent heat changes due to hemin transfer the Hb was maintained in the carbonmonoxy ligated state and hemin binding deficient receptor proteins containing an alanine substitution for Y642. The HbCO and the apo-receptor proteins were buffer matched in ITC buffer (20 mM NaH₂PO₄, 150 mM NaCl, 0.45M sucrose, pH 7.5). The cell was filled with 30 µM HbCO and the syringe was filled with 200, 300, and 850 $\mu M \alpha$ -IsdH^{Y642A}, α -IsdH^{N2}, IsdH^{LN3(Y642A)}, respectively. Twenty injections were performed using 2.0 µL injection volumes at 180 s intervals. ORIGIN software was used to fit the data to a single-site binding model. The heat (Q) is related to the number of sites (n), the binding constant (K), and the enthalpy (ΔH) via the following equation,

$$Q = \frac{n M_t \Delta H V_{\rm o}}{2} \left[1 + \frac{X_t}{n M_t} + \frac{1}{n K M_t} - \sqrt{(1 + \frac{X_t}{n M_t} + \frac{1}{n K M_t})^2 - \frac{4 X_t}{n M_t}} \right]$$

where X_t , M_t , and V_o represent the bulk concentration of ligand, the bulk concentration of macromolecule in V_o , and the active cell volume respectively. A correction is made to account for the displaced volume after the ith injection,

$$\Delta Q(i) = Q(i) + \frac{dV_i}{V_o} \left[\frac{Q(i) + Q(i-1)}{2} \right] - Q(i-1)$$

Calculated $\Delta Q(i)$ values for each injection are compared to the corresponding experimental values. The fit is improved over successive iterations by altering values for n, K, and ΔH (74).

Molecular dynamic simulations. The protein structure for the IsdH-bound system was taken directly from a methemoglobin dimer-IsdH complex (PDB 4XS0, resolution 2.55 Å (31)),

while the coordinates of native methemoglobin was taken from a tetramer deoxy-hemoglobin structure (PDB 1A3N, resolution 1.8 Å (75)). Missing residues in each structure were added using ModLoop (76). Both systems were neutralized with Na⁺ ions and solvated with TIP3P (77) waters and a 150 mM NaCl environment in a periodic box, which had a minimum of 10 Å from protein heavy atoms to the box edge. Following minimization for 4,500 steps, both systems were heated to 300K with restraints of 10 kcal/mol/Å² on the solute heavy atoms applied for 20 ps, and the restraints were then gradually removed over 350 ps. Production simulations of 200 ns were then performed in the NPT ensemble with temperature maintained via a Langevin thermostat and pressure regulated with a Berendsen barostat (78). Nonbonded interactions were truncated at 10 Å, and long ranged electrostatics were computed with the particle-mesh Ewald method using a

maximum spacing of 1.0 Å. All simulations were performed with the GPU accelerated version of PMEMD in the Amber16 package (79). The AMBERff14SB force field was used for the proteins, while parameters for hemin and the N_ε-Fe³⁺ bond were calculated following the protocol of Shahrokh et al (80). In short, geometry optimization, frequency calculations, electrostatic potential calculations were done in Gaussian09 (81), and a RESP fit was performed in antechamber Gaussian and tleap scripts were generated using MCBP.py from AmberTools16. Bonded and van der Waals parameters were derived from the General Amber Force Field (GAFF)(82). Analysis of each system was performed on the final 150 ns of simulations using VMD (83), MDAnalysis (84), and CPPTRAJ (85). The GIST analysis was done with a grid spanning 33x41x61 Å and a grid spacing of 0.5 Å.

Acknowledgements: We thank Dr. Robert Peterson for assistance with the NMR experiments. This work was supported by National Science Foundation Grant MCB-1716948 (to R.T.C. and J.W.) and National Institutes of Health Grants AI52217 (to R.T.C.), R35GM119647 (to J.W.), F31GM101931 (to M.S.) and P01-HL110900 (to J.S.O.). J.S.O. was also supported by a grant from the Robert A. Welch Foundation (C-0612). R.M. was supported by a Cellular and Molecular Biology Training Grant (Ruth L. Kirschstein National Research Service Award GM007185). NMR equipment used in this research was purchased using funds from shared equipment grant NIH S10OD016336.

Conflict of Interest: The authors declare that they have no conflicts of interest with the contents of this article.

Author contributions: MS conducted the hemin transfer experiments, analyzed the results, and wrote a significant portion of the paper. RM performed the isothermal titration calorimetry experiments, and analyzed these results. JMD assisted with the hemin transfer experiments. JD and JW performed the molecular dynamics simulations and analyzed the results. JSO assisted with the hemin transfer experiments, provided key reagents and helped design the experimental procedure. MP conducted the analytical ultracentrifugation experiments and analyzed the data. DAG provided essential experimental experimental experimental data, and wrote the paper with MS.

REFERENCES

- 1. Klevens, R. M., Morrison, M. A., Nadle, J., Petit, S., Gershman, K., Ray, S., Harrison, L. H., Lynfield, R., Dumyati, G., Townes, J. M., Craig, A. S., Zell, E. R., Fosheim, G. E., McDougal, L. K., Carey, R. B., Fridkin, S. K., and Active Bacterial Core surveillance (ABCs) MRSA Investigators (2007) Invasive methicillin-resistant Staphylococcus aureus infections in the United States. *JAMA*. **298**, 1763–71
- 2. Centers for Disease Control and Prevention (2013) Active Bacterial Core Surveillance (ABCs) Report Emerging Infections Program Network Methicillin-Resistant Staphylococcus aureus, 2013
- 3. Dukic, V. M., Lauderdale, D. S., Wilder, J., Daum, R. S., and David, M. Z. (2013) Epidemics of community-associated methicillin-resistant Staphylococcus aureus in the United States: a meta-analysis. *PLoS One.* **8**, e52722
- 4. Ong, S. T., Ho, J. Z. S., Ho, B., and Ding, J. L. (2006) Iron-withholding strategy in innate immunity. *Immunobiology*. **211**, 295–314
- 5. Haley, K. P. P., and Skaar, E. P. P. (2012) A battle for iron: host sequestration and Staphylococcus aureus acquisition. *Microbes Infect.* **14**, 217–227
- 6. Farrand, A. J., Reniere, M. L., Ingmer, H., Frees, D., and Skaar, E. P. (2013) Regulation of Host Hemoglobin Binding by the Staphylococcus aureus Clp Proteolytic System. *J. Bacteriol.* **195**, 5041–5050
- 7. Skaar, E. P., Humayun, M., Bae, T., DeBord, K. L., and Schneewind, O. (2004) Ironsource preference of Staphylococcus aureus infections. *Science*. **305**, 1626–8
- 8. Mazmanian, S. K., Skaar, E. P., Gaspar, A. H., Humayun, M., Gornicki, P., Jelenska, J., Joachmiak, A., Missiakas, D. M., and Schneewind, O. (2003) Passage of heme-iron across the envelope of Staphylococcus aureus. *Science*. **299**, 906–9
- 9. Maresso, A. W., and Schneewind, O. (2006) Iron acquisition and transport in Staphylococcus aureus. *Biometals*. **19**, 193–203
- 10. Reniere, M. L., Torres, V. J., and Skaar, E. P. (2007) Intracellular metalloporphyrin metabolism in Staphylococcus aureus. *Biometals*. **20**, 333–45
- 11. Mazmanian, S. K., Ton-That, H., Su, K., and Schneewind, O. (2002) An iron-regulated sortase anchors a class of surface protein during Staphylococcus aureus pathogenesis. *Proc. Natl. Acad. Sci.* **99**, 2293–2298

- 12. Ton-That, H., Marraffini, L. A., and Schneewind, O. (2004) Protein sorting to the cell wall envelope of Gram-positive bacteria. *Biochim. Biophys. Acta.* **1694**, 269–78
- 13. Pilpa, R. M., Robson, S. A., Villareal, V. A., Wong, M. L., Phillips, M., and Clubb, R. T. (2009) Functionally distinct NEAT (NEAr Transporter) domains within the Staphylococcus aureus IsdH/HarA protein extract heme from methemoglobin. *J. Biol. Chem.* **284**, 1166–76
- 14. Pishchany, G., Sheldon, J. R., Dickson, C. F., Alam, M. T., Read, T. D., Gell, D. A., Heinrichs, D. E., and Skaar, E. P. (2014) IsdB-dependent Hemoglobin Binding Is Required for Acquisition of Heme by Staphylococcus aureus. *J. Infect. Dis.* **209**, 1764–72
- 15. Spirig, T., Malmirchegini, G. R., Zhang, J., Robson, S. A., Sjodt, M., Liu, M., Krishna Kumar, K., Dickson, C. F., Gell, D. A., Lei, B., Loo, J. a, Clubb, R. T. (2013) Staphylococcus aureus uses a novel multidomain receptor to break apart human hemoglobin and steal its heme. *J. Biol. Chem.* **288**, 1065–78
- 16. Zhu, H., Li, D., Liu, M., Copié, V., and Lei, B. (2014) Non-Heme-Binding Domains and Segments of the Staphylococcus aureus IsdB Protein Critically Contribute to the Kinetics and Equilibrium of Heme Acquisition from Methemoglobin. *PLoS One.* **9**, e100744
- 17. Dryla, A., Gelbmann, D., Von Gabain, A., and Nagy, E. (2003) Identification of a novel iron regulated staphylococcal surface protein with haptoglobin-haemoglobin binding activity. *Mol. Microbiol.* **49**, 37–53
- 18. Pishchany, G., Dickey, S. E., and Skaar, E. P. (2009) Subcellular localization of the Staphylococcus aureus heme iron transport components IsdA and IsdB. *Infect. Immun.* **77**, 2624–34
- 19. Villareal, V. a, Spirig, T., Robson, S. A., Liu, M., Lei, B., and Clubb, R. T. (2011) Transient weak protein-protein complexes transfer heme across the cell wall of Staphylococcus aureus. *J. Am. Chem. Soc.* **133**, 14176–9
- 20. Abe, R., Caaveiro, J. M. M., Kozuka-Hata, H., Oyama, M., and Tsumoto, K. (2012) Mapping Ultra-weak Protein-Protein Interactions between Heme Transporters of Staphylococcus aureus. *J. Biol. Chem.* **287**, 16477–16487
- 21. Muryoi, N., Tiedemann, M. T., Pluym, M., Cheung, J., Heinrichs, D. E., and Stillman, M. J. (2008) Demonstration of the iron-regulated surface determinant (Isd) heme transfer pathway in Staphylococcus aureus. *J. Biol. Chem.* **283**, 28125–36
- 22. Zhu, H., Xie, G., Liu, M., Olson, J. S., Fabian, M., Dooley, D. M., and Lei, B. (2008) Pathway for heme uptake from human methemoglobin by the iron-regulated surface determinants system of Staphylococcus aureus. *J. Biol. Chem.* **283**, 18450–60

- 23. Matsui, T., Nambu, S., Ono, Y., Goulding, C. W., Tsumoto, K., and Ikeda-Saito, M. (2013) Heme degradation by Staphylococcus aureus IsdG and IsdI liberates formaldehyde rather than carbon monoxide. *Biochemistry*. **52**, 3025–7
- 24. Reniere, M. L., Ukpabi, G. N., Harry, S. R., Stec, D. F., Krull, R., Wright, D. W., Bachmann, B. O., Murphy, M. E., and Skaar, E. P. (2010) The IsdG-family of haem oxygenases degrades haem to a novel chromophore. *Mol. Microbiol.* **75**, 1529–38
- 25. Torres, V. J., Pishchany, G., Humayun, M., Schneewind, O., and Skaar, E. P. (2006) Staphylococcus aureus IsdB is a hemoglobin receptor required for heme iron utilization. *J. Bacteriol.* **188**, 8421–9
- 26. Pishchany, G., McCoy, A. L., Torres, V. J., Krause, J. C., Crowe, J. E., Fabry, M. E., and Skaar, E. P. (2010) Specificity for human hemoglobin enhances Staphylococcus aureus infection. *Cell Host Microbe*. **8**, 544–50
- 27. Kim, H. K., DeDent, A., Cheng, A. G., McAdow, M., Bagnoli, F., Missiakas, D. M., and Schneewind, O. (2010) IsdA and IsdB antibodies protect mice against Staphylococcus aureus abscess formation and lethal challenge. *Vaccine*. **28**, 6382–92
- 28. Fonner, B. A., Tripet, B. P., Eilers, B., Stanisich, J., Sullivan-Springhetti, R. K., Moore, R., Liu, M., Lei, B., and Copie, V. (2014) Solution Structure and Molecular determinants of Hemoglobin Binding of the first NEAT Domain of IsdB in Staphylococcus aureus. *Biochemistry*. **53**, 3922–3933
- 29. Sjodt, M., Macdonald, R., Spirig, T., Chan, A. H., Dickson, C. F., Fabian, M., Olson, J. S., Gell, D. A., and Clubb, R. T. (2016) The PRE-Derived NMR Model of the 38.8-kDa Tri-Domain IsdH Protein from Staphylococcus aureus Suggests That It Adaptively Recognizes Human Hemoglobin. *J. Mol. Biol.* **428**, 1107–1129
- 30. Dickson, C. F., Kumar, K. K., Jacques, D. A., Malmirchegini, G. R., Spirig, T., Mackay, J. P., Clubb, R. T., Guss, J. M., Gell, D. A. (2014) Structure of the Hemoglobin-IsdH Complex Reveals the Molecular Basis of Iron Capture by Staphylococcus aureus. *J. Biol. Chem.* **289**, 6728–6738
- 31. Dickson, C. F., Jacques, D. A., Clubb, R. T., Guss, J. M., and Gell, D. A. (2015) The structure of haemoglobin bound to the haemoglobin receptor IsdH from Staphylococcus aureus shows disruption of the native α-globin haem pocket. *Acta Crystallogr. Sect. D Biol. Crystallogr.* 10.1107/S1399004715005817
- 32. Andrade, M., Ciccarelli, F., Perez-Iratxeta, C., and Bork, P. (2002) NEAT: a domain duplicated in genes near the components of a putative Fe3+ siderophore transporter from Gram-positive pathogenic bacteria. *Genome Biol.* 3, research0047.1–research0047.5

- 33. Bowden, C. F., Verstraete, M. M., Eltis, L. D., and Murphy, M. E. P. (2014) Hemoglobin binding and catalytic heme extraction by IsdB NEAT domains. *Biochemistry*. **53**, 2286–2294
- 34. Benesch, R. E., and Kwong, S. (1995) Coupled reactions in hemoglobin. Heme-globin and dimer-dimer association. *J. Biol. Chem.* **270**, 13785–6
- 35. Hargrove, M. S., Whitaker, T., Olson, J. S., Vali, R. J., and Mathews, A. J. (1997) Quaternary Structure Regulates Hemin Dissociation from Human Hemoglobin. *J. Biol. Chem.* **272**, 17385–17389
- 36. Bunn, H. F., and Jandl, J. H. (1968) Exchange of heme among hemoglobins and between hemoglobin and albumin. *J. Biol. Chem.* **243**, 465–75
- 37. Gattoni, M., Boffi, A., Sarti, P., and Chiancone, E. (1996) Stability of the heme-globin linkage in alphabeta dimers and isolated chains of human hemoglobin. A study of the heme transfer reaction from the immobilized proteins to albumin. *J. Biol. Chem.* **271**, 10130–6
- 38. Leutzinger, Y., and Beychok, S. (1981) Kinetics and mechanism of heme-induced refolding of human alpha-globin. *Proc. Natl. Acad. Sci. U. S. A.* **78**, 780–4
- 39. Hargrove, M. S., Singleton, E. W., Quillin, M. L., Ortiz, L. A., Phillips, G. N., Olson, J. S., and Mathews, A. J. (1994) His64(E7)-->Tyr apomyoglobin as a reagent for measuring rates of hemin dissociation. *J. Biol. Chem.* **269**, 4207–14
- 40. Looker, D., Abbott-Brown, D., Cozart, P., Durfee, S., Hoffman, S., Mathews, A. J., Miller-Roehrich, J., Shoemaker, S., Trimble, S., Fermi, G., Miller-Roehrkh, J., Shoemaker, S., Trimble, S., Fermi, G., Komiyama, N. H., Nagai, K., and Stetler, G. L. (1992) A human recombinant haemoglobin designed for use as a blood substitute. *Nature*. **356**, 258–60
- 41. Watanabe, M., Tanaka, Y., Suenaga, A., Kuroda, M., Yao, M., Watanabe, N., Arisaka, F., Ohta, T., Tanaka, I., and Tsumoto, K. (2008) Structural basis for multimeric heme complexation through a specific protein-heme interaction: the case of the third neat domain of IsdH from Staphylococcus aureus. *J. Biol. Chem.* **283**, 28649–28659
- 42. Krishna Kumar, K., Jacques, D. A., Pishchany, G., Caradoc-Davies, T., Spirig, T., Malmirchegini, G. R., Langley, D. B., Dickson, C. F., Mackay, J. P., Clubb, R. T., Skaar, E. P., Guss, J. M., and Gell, D. A. (2011) Structural basis for hemoglobin capture by Staphylococcus aureus cell-surface protein, IsdH. *J. Biol. Chem.* **286**, 38439–47
- 43. McGovern, P., Reisberg, P., and Olson, J. S. (1976) Aggregation of deoxyhemoglobin subunits. *J. Biol. Chem.* **251**, 7871–9
- 44. Espenson, J. H. (1995) Chemical Kinetics and Reaction Mechanisms, McGraw-Hill

- 45. Pilpa, R. M., Fadeev, E. A., Villareal, V. A., Wong, M. L., Phillips, M., and Clubb, R. T. (2006) Solution structure of the NEAT (NEAr Transporter) domain from IsdH/HarA: the human hemoglobin receptor in Staphylococcus aureus. *J. Mol. Biol.* **360**, 435–47
- 46. Sheldon, J. R., and Heinrichs, D. E. (2015) Recent developments in understanding the iron acquisition strategies of gram positive pathogens. *FEMS Microbiol. Rev.* **39**, 592–630
- 47. Perutz, M. F. (1979) Regulation of oxygen affinity of hemoglobin: influence of structure of the globin on the heme iron. *Annu. Rev. Biochem.* **48**, 327–86
- 48. Liong, E. C., Dou, Y., Scott, E. E., Olson, J. S., and Phillips, G. N. (2001) Waterproofing the heme pocket. Role of proximal amino acid side chains in preventing hemin loss from myoglobin. *J. Biol. Chem.* **276**, 9093–100
- 49. Hargrove, M. S., Barrick, D., and Olson, J. S. (1996) The association rate constant for heme binding to globin is independent of protein structure. *Biochemistry*. **35**, 11293–9
- 50. Rose, M. Y., and Olson, J. S. (1983) The kinetic mechanism of heme binding to human apohemoglobin. *J. Biol. Chem.* **258**, 4298–303
- 51. Makowski, L., Bardhan, J., Gore, D., Lal, J., Mandava, S., Park, S., Rodi, D. J., Ho, N. T., Ho, C., and Fischetti, R. F. (2011) WAXS Studies of the Structural Diversity of Hemoglobin in Solution. *J. Mol. Biol.* 408, 909–921
- 52. Abaturov, L. V, Nosova, N. G., Shliapnikov, S. V, and Faĭzullin, D. A. The conformational dynamic of the tetramer hemoglobin molecule as revealed by hydrogen exchange. I. Influence pH, temperature and ligand binding. *Mol. Biol. (Mosk).* **40**, 326–40
- 53. Kawamura-Konishi, Y., Chiba, K., Kihara, H., and Suzuki, H. (1992) Kinetics of the reconstitution of hemoglobin from semihemoglobins alpha and beta with heme. *Eur. Biophys. J.* **21**, 85–92
- 54. Dickson, C. F., Rich, A. M., D'Avigdor, W. M. H., Collins, D. A. T., Lowry, J. A., Mollan, T. L., Khandros, E., Olson, J. S., Weiss, M. J., Mackay, J. P., Lay, P. A., and Gell, D. A. (2013) α-Hemoglobin-stabilizing protein (AHSP) perturbs the proximal heme pocket of oxy-α-hemoglobin and weakens the iron-oxygen bond. *J. Biol. Chem.* 288, 19986–20001
- 55. Krishna Kumar, K., Dickson, C. F. F., Weiss, M. J. J., Mackay, J. P. P., Gell, D. A. (2010) AHSP (α-haemoglobin-stabilizing protein) stabilizes apo-α-haemoglobin in a partially folded state. *Biochem. J.* **432**, 275–82
- 56. Zhou, S., Olson, J. S., Fabian, M., Weiss, M. J., and Gow, A. J. (2006) Biochemical fates of alpha hemoglobin bound to alpha hemoglobin-stabilizing protein AHSP. *J. Biol. Chem.* **281**, 32611–8

- 57. Sæderup, K. L., Stødkilde, K., Graversen, J. H., Dickson, C. F., Etzerodt, A., Hansen, S. W. K., Fago, A., Gell, D., Andersen, C. B. F., and Moestrup, S. K. (2016) The Staphylococcus aureus Protein IsdH inhibits host hemoglobin scavenging to promote heme acquisition by the pathogen. *J. Biol. Chem.* **291**, 23989–23998
- 58. Dryla, A., Hoffmann, B., Gelbmann, D., Giefing, C., Hanner, M., Meinke, A., Anderson, A. S., Koppensteiner, W., Konrat, R., Von Gabain, A., and Nagy, E. (2007) High-affinity binding of the staphylococcal HarA protein to haptoglobin and hemoglobin involves a domain with an antiparallel eight-stranded β-barrel fold. *J. Bacteriol.* **189**, 254–264
- 59. Mollan, T. L., Jia, Y., Banerjee, S., Wu, G., Timothy Kreulen, R., Tsai, A. L., Olson, J. S., Crumbliss, A. L., and Alayash, A. I. (2014) Redox properties of human hemoglobin in complex with fractionated dimeric and polymeric human haptoglobin. *Free Radic. Biol. Med.* **69**, 265–277
- 60. Krishnamurthy, V. M., Semetey, V., Bracher, P. J., Shen, N., and Whitesides, G. M. (2007) Dependence of effective molarity on linker length for an intramolecular protein-ligand system. *J. Am. Chem. Soc.* **129**, 1312–20
- 61. Harrington, J. P., Newton, P., Crumpton, T., and Keaton, L. (1993) Induced hemichrome formation of methemoglobins A, S and F by fatty acids, alkyl ureas and urea. *Int. J. Biochem.* **25**, 665–670
- 62. Bowden, C. F. M., Chan, A. C. K., Li, E. J. W., Arrieta, A. L., Eltis, L. D., and Murphy, M. E. P. (2018) Structure-function analyses reveal key features in Staphylococcus aureus IsdB-associated unfolding of the heme-binding pocket of human hemoglobin. *J. Biol. Chem.* **293**, 177–190
- 63. Samuel, P. P., Ou, W. C., Phillips, G. N., and Olson, J. S. (2017) Mechanism of Human Apohemoglobin Unfolding. *Biochemistry*. **56**, 1444–1459
- 64. Senturia, R., Faller, M., Yin, S., Loo, J. A., Cascio, D., Sawaya, M. R., Hwang, D., Clubb, R. T., and Guo, F. (2010) Structure of the dimerization domain of DiGeorge critical region 8. *Protein Sci.* **19**, 1354–65
- 65. Reverter, D., and Lima, C. D. (2004) A basis for SUMO protease specificity provided by analysis of human Senp2 and a Senp2-SUMO complex. *Structure*. **12**, 1519–31
- 66. Spirig, T., and Clubb, R. T. (2012) Backbone (1)H, (13)C and (15)N resonance assignments of the 39 kDa staphylococcal hemoglobin receptor IsdH. *Biomol. NMR Assign.* **6**, 169–172
- 67. Ascoli, F., Fanelli, M. R., and Antonini, E. (1981) Preparation and properties of apohemoglobin and reconstituted hemoglobins. *Methods Enzymol.* **76**, 72–87

- 68. Gell, D., Kong, Y., Eaton, S. a, Weiss, M. J., and Mackay, J. P. (2002) Biophysical characterization of the alpha-globin binding protein alpha-hemoglobin stabilizing protein. *J. Biol. Chem.* **277**, 40602–9
- 69. Looker, D., Mathews, A. J., Neway, J. O., and Stetler, G. L. (1994) Expression of recombinant human hemoglobin in Escherichia coli. *Methods Enzymol.* **231**, 364–74
- 70. Manning, J. M. (1981) [14] Preparation of hemoglobin carbamylated at specific NH2-terminal residues. *Methods Enzymol.* **76**, 159–167
- 71. Antonini E. & Brunori M. (1971) Hemoglobin and Myoglobin in their Reactions with Ligands,. *Amsterdam, Netherlands North-holl*.
- 72. Cohn, E. J. & Edsall, J. T. (1943) *Proteins, Amino Acids and Peptides as Ions and Dipolar Ions (Cohn, Edwin J.; Edsall, John T.)* (Cohn, E. J. & Edsall, J. T. ed), Reinhold Publishing Corporation, New York
- 73. Laue, T., Shah, B., Ridgeway, T., and Pelletier, S. (1992) Computer-aided interpretation of analytical sedimentation data for proteins. in *Analytical Ultracentrifugation in Biochemistry and Polymer Science* (Harding SE, Rowe AJ, H. J. ed), pp. 90–125, Cambridge: The Royal Society of Chemistry
- 74. Malvern Instruments Limited (2014) Microcal ITC200 system User Manual
- 75. Tame, J. R. H., and Vallone, B. (2000) The structures of deoxy human haemoglobin and the mutant Hb Tyrα42His at 120 K. *Acta Crystallogr. Sect. D Biol. Crystallogr.* **56**, 805–811
- 76. Fiser, A., and Sali, A. (2003) ModLoop: Automated modeling of loops in protein structures. *Bioinformatics*. **19**, 2500–2501
- 77. Jorgensen, W. L., Chandrasekhar, J., Madura, J. D., Impey, R. W., and Klein, M. L. (1983) Comparison of simple potential functions for simulating liquid water. *J. Chem. Phys.* **79**, 926–935
- 78. Berendsen, H. J. C., Postma, J. P. M., van Gunsteren, W. F., DiNola, A., and Haak, J. R. (1984) Molecular dynamics with coupling to an external bath. *J. Chem. Phys.* **81**, 3684–3690
- 79. D.A. Case W. Botello-Smith, D.S. Cerutti, T.E. Cheatham, III, T.A. Darden, R.E. Duke, T.J. Giese, H. Gohlke, A.W. Goetz, N. Homeyer, S. Izadi, P. Janowski, J. Kaus, A. Kovalenko, T.S. Lee, S. LeGrand, P. Li, C. Lin, T. Luchko, R. Luo, B. Madej, D.M. York, R. M. B. (2016) *AMBER 16*

- 80. Shahrokh, K., Orendt, A., Yost, G. S., and Cheatham, T. E. (2012) Quantum mechanically derived AMBER-compatible heme parameters for various states of the cytochrome P450 catalytic cycle. *J. Comput. Chem.* **33**, 119–133
- Frisch, M. J., Trucks, G. W., Schlegel, H. B., Scuseria, G. E., Robb, M. A., Cheeseman, J. R., Scalmani, G., Barone, V., Mennucci, B., Petersson, G. A., Nakatsuji, H., Caricato, M., Li, X., Hratchian, H. P., Izmaylov, A. F., Bloino, J., Zheng, G., Sonnenberg, J. L., Hada, M., Ehara, M., Toyota, K., Fukuda, R., Hasegawa, J., Ishida, M., Nakajima, T., Honda, Y., Kitao, O., Nakai, H., Vreven, T., Montgomery Jr., J. A., Peralta, J. E., Ogliaro, F., Bearpark, M., Heyd, J. J., Brothers, E., Kudin, K. N., Staroverov, V. N., Kobayashi, R., Normand, J., Raghavachari, K., Rendell, A., Burant, J. C., Iyengar, S. S., Tomasi, J., Cossi, M., Rega, N., Millam, J. M., Klene, M., Knox, J. E., Cross, J. B., Bakken, V., Adamo, C., Jaramillo, J., Gomperts, R., Stratmann, R. E., Yazyev, O., Austin, A. J., Cammi, R., Pomelli, C., Ochterski, J. W., Martin, R. L., Morokuma, K., Zakrzewski, V. G., Voth, G. A., Salvador, P., Dannenberg, J. J., Dapprich, S., Daniels, A. D., Farkas, O., Foresman, J. B., Ortiz, J. V, Cioslowski, J., and Fox, D. J. (2010) Gaussian09 Revision D.01, Gaussian Inc. Wallingford CT. Gaussian 09 Revis. C.01. 10.1017/CBO9781107415324.004
- Wang, J., Wolf, R. M., Caldwell, J. W., Kollman, P. A., and Case, D. A. (2004)
 Development and testing of a general Amber force field. *J. Comput. Chem.* **25**, 1157–1174
- 83. Humphrey, W., Dalke, A., and Schulten, K. (1996) VMD: Visual molecular dynamics. *J. Mol. Graph.* **14**, 33–38
- 84. Michaud-Agrawal, N., Denning, E. J., Woolf, T. B., and Beckstein, O. (2011) MDAnalysis: A toolkit for the analysis of molecular dynamics simulations. *J. Comput. Chem.* **32**, 2319–2327
- 85. Roe, D. R., and Cheatham, T. E. (2013) PTRAJ and CPPTRAJ: Software for processing and analysis of molecular dynamics trajectory data. *J. Chem. Theory Comput.* **9**, 3084–3095

 Table 1
 Stoichiometry of Hb:receptor complexes determined by analytical ultracentrifugation

	Weighted average molecular masses (Da) ^{a,b}	Receptor/globin
Hb0.1 ^c		
$13,000 \times g$	$64,212 \pm 829$	
$\mathbf{Hb0.1} + \alpha \mathbf{-IsdH}^{\mathbf{Y642A}c,d}$		
$6,000 \times g$	$140,070 \pm 2096$	2.0
$13,000 \times g$	$131,570 \pm 894$	1.7
$\mathbf{Hb0.1} + \alpha \cdot \mathbf{IsdH}^{\mathbf{Y642A}c,e}$		
$6,000 \times g$	$134,660 \pm 1,872$	1.8
$13,000 \times g$	$128,490 \pm 1115$	1.7
$\mathbf{Hb0.1} + \mathbf{IsdH}^{\mathbf{Y642A}c,e}$		
$6,000 \times g$	$188,110 \pm 1,518$	3.2
$13,000 \times g$	$175,120 \pm 1045$	2.9
$β$ -globin c		
$6,000 \times g$	$56,700 \pm 724$	
$13,000 \times g$	$56,300 \pm 508$	
β -globin + α -IsdH Y642Ac,e		
$6,000 \times g$	$54,500 \pm 97$	0.0
$13,000 \times g$	$54,500 \pm 65$	0.0
β -globin + IsdH Y642Ac,e		
$6,000 \times g$	$134,000 \pm 1321$	2.0
$13,000 \times g$	$116,500 \pm 617$	1.6

^a Samples were centrifuged at 25°C in buffer containing 20 mM sodium phosphate, 150 mM NaCl, 450 mM sucrose, pH 7.5

^b Molecular masses were obtained by non-linear least squares exponential fitting of data using Beckman Origin-based software (Version 3.01)

^c Globin chains were held at a concentration of 5 μM (hemin units)

^d Receptor concentrations were in a 15-fold molar excess (75 μM)

^e Receptor concentrations were in a 30-fold molar excess (150 μM)

 Table 2
 Apparent rate constants of hemin transfer

Hemin donor	Hemin acceptor	$k_{\mathrm{fast}} (\mathrm{s}^{\text{-}1})^{\mathrm{a}}$	$k_{\mathrm{slow}} (\mathrm{s}^{\text{-}1})^{\mathrm{a}}$
MetHb	α -IsdH b	3.27 ± 0.07	0.038 ± 0.001
	IsdH^b	3.12 ± 0.08	0.039 ± 0.001
	apo-Mb ^{c,d}	$0.004^{e} (0.01)^{f}$	$0.0002^{e} (0.003)^{f}$
MetHb0.1	apo-Mb ^{c,d} α- IsdH ^b	0.34 ± 0.01	0.026 ± 0.001
	$IsdH^b$	0.73 ± 0.03	0.041 ± 0.001
	$apo-Mb^{c,d}$	0.0004^{g}	0.00008^g

 $^{^{}a}k_{\text{fast}}$ and k_{slow} values were obtained by fitting to a double exponential expression.

^b Rates were determined at a 30-fold excess [Receptor] pH 7.5, 25°C.

^c Rates were determined at pH 7.0, 37°C.

^d The data are from Ref. (35).

 $^{^{}e}$ k_{fast} and k_{slow} are from the β- and α-globin chains in dimeric Hb, respectively.

 $f_{k_{\text{fast}}}$ and k_{slow} are from the β- and α-globin chains in monomeric Hb, respectively.

 $[^]g$ k_{fast} and k_{slow} are from the β- and α-globin chains in tetrameric Hb, respectively. These values are also the same for tetrameric wild-type Hb.

Table 3 Thermodynamic parameters and affinity data for Hb binding

	K_{D}	ΔH°	ΔS°	ΔG°^a}	n ^b
	μM	kcal/mol	cal/mol·K	kcal/mol	
$Hb + \alpha IsdH^{Y642A}$	4.0 ± 0.6	-6.0 ± 0.5	4.6 ± 1.9	-7.4 ± 0.1	0.59 ± 0.03
$Hb + \alpha IsdH^{N2}$	7.5 ± 1.1	-10.3 ± 0.5	-11.1 ± 2.0	-7.0 ± 0.1	0.62 ± 0.04
$Hb + \alpha IsdH^{LN3(Y642A)}$	\geq mM	endothermic	positive	ND^c	ND

^a Samples were in buffer containing 20 mM sodium phosphate, 150 mM NaCl, 450 mM sucrose, pH 7.5, 298K ^bn refers to the molar ratio protein:Hb. ^c ND refers to "not determined".

Errors represent the standard deviation of four replicates.

FIGURE LEGENDS

Figure 1. *S. aureus* uses conserved tridomain containing receptors to capture Hb. (a) Schematic showing the domain organization within the *S. aureus* Hb receptors, IsdH and IsdB. NEAT domains (N) that bind Hb and hemin (oxidized form of heme) are shown in gray and black, respectively. The helical domain that connects them is labeled "linker". Residue numbers that define the boundaries of the functionally homologous NEAT domains are indicated. (b) Crystal structure of the Hb:α-IsdH^{N2N3} complex (pdb 4XSO) with only contacts to the α-subunit shown. Proteins are shown in ribbon format, while the hemin group is represented by a space filling model. Density for residues in the segment connecting the N2 and linker domains are absent in the electron density (dashed line). (c) Close up view of the LN3-Hb interface that is distorted. α-IsdH is shown in blue and ribbon diagram of αHb is shown in yellow (α-IsdH, residues A326-D660 from IsdH containing 365 FYHYA $^{369} \rightarrow ^{365}$ YYHYF 369 mutations). The F-helix in the receptor-Hb complex that is distorted (colored red) is overlaid with the native F-helix observed in the isolated Hb protein (colored green) (PDB code: 2DN2). The hemin group is represented by a space filling model (grey) with the iron atom colored red.

Figure 2. Stoichiometry of Hb:receptor complexes determined by analytical ultracentrifugation. (a) Representative absorbance scans at 412 nm at equilibrium are plotted versus the distance from the axis of rotation for a mixture of Hb0.1 + IsdH Y642A (blue circles) and Hb0.1 + α-IsdH Y642A (red triangles). Hb0.1 was maintained in the carbonmonoxy ligated state, and both receptors contained Y642A mutation to prevent heme transfer. Protein samples were mixed at a ratio of 5 μM Hb0.1 and 150 μM receptor and were centrifuged at 25 °C for at least 48 h at 13,000 rpm. The solid lines represent the global nonlinear least squares best-fit of all the data to a single molecular species with a baseline fit. Residuals of the fit are shown above each panel. (b) Representative scans identical to the conditions described in (a) with the exception that 5 μM β-CO (isolated β-chains) was used and samples were centrifuged at a speed of 9,000 rpm.

Figure 3. Hemin transfer by various Hb and receptors species. (a) Spectral changes in the UV–Vis spectrum of the reaction containing 5 μM Hb0.1 with buffer (solid black line), 150 μM IsdH^{N2N3} (dotted blue line), and 150 μM α-IsdH (solid red line). Spectral traces were recorded at 1000 s post mixing. (b) Representative stopped-flow time courses showing absorbance changes at 405 nm (ΔA_{405}) after mixing 5 μM Hb or Hb0.1 with 150 μM apo-receptor. The data were fit to a double-exponential equation to obtain k_{fast} and k_{slow} hemin transfer rates. Spectral traces were normalized for comparison using the following equation: $y = (y_t - y_0) / (y_t + y_0)$. Panels (c) and (d) show the measured k_{fast} and k_{slow} rate constants, respectively. Values were derived from the time courses in (b). A two-way ANOVA was used to access the significance in the difference of rates. NS and *** corresponds to p-values > 0.05 and < 0.001, respectively.

Figure 4. Hemin transfer from isolated β-globin chains. Representative stopped-flow time courses showing absorbance changes at 408 nm (ΔA_{408}) after mixing 5 μM isolated Metβ-globin chains with 150 μM apo-receptor or 50 μM apo-Mb. Relative spectral traces are shown for comparison in which all starting absorbance were normalized to a value of 1. Only the first 10 s are shown as absorbance artifacts were observed after this time as a result of the slow process of apo-globin denaturation.

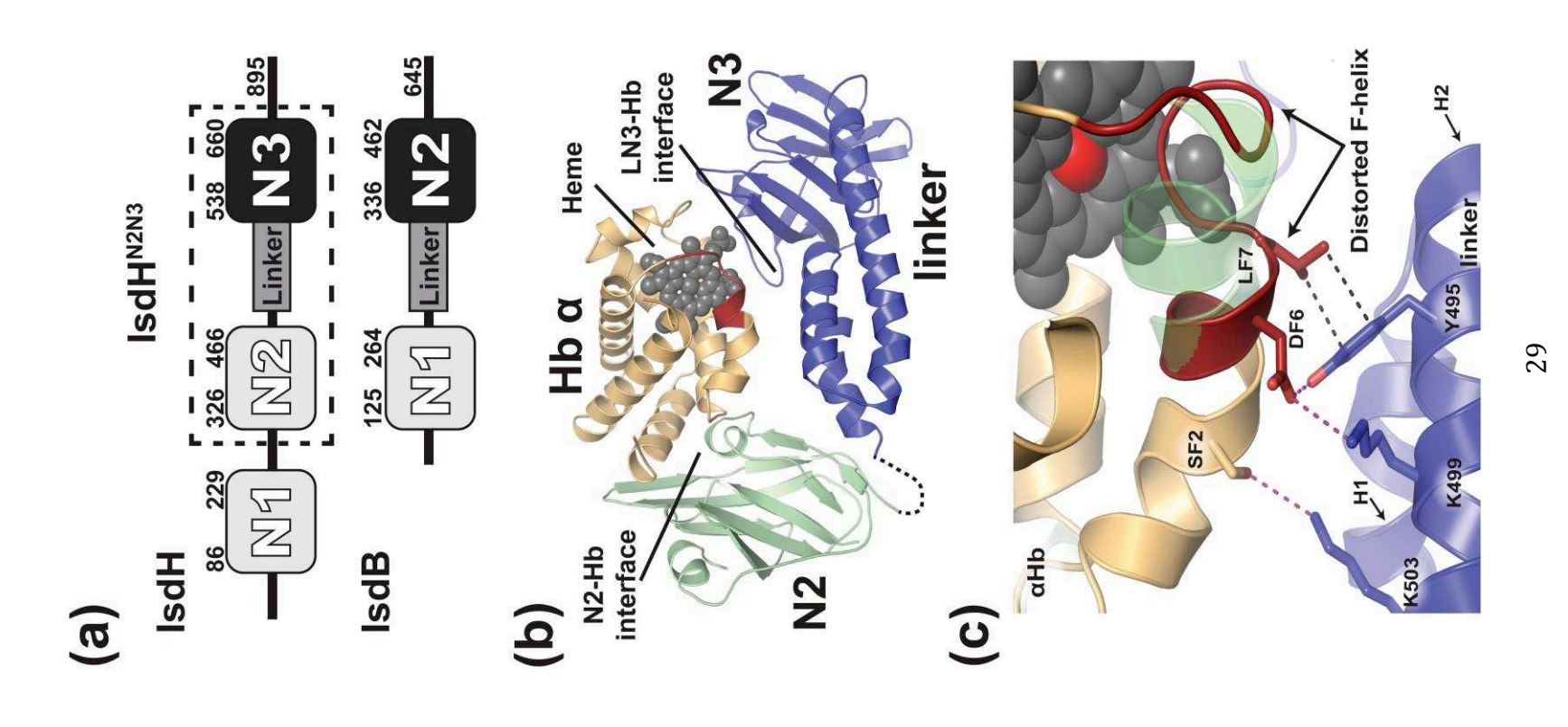
Figure 5. Hemin transfer to myoglobin and as function of receptor concentration. (a) Spontaneous hemin release from the receptor and Hb was measured using H64Y/V68F apomyoglobin. Time courses of the absorbance change at 600 nm (ΔA_{600}) of a mixture of H64Y/V68F apomyoglobin (Mb) with Hb (black line), Hb0.1 (dark grey line), and IsdH^{N2N3} (light grey line) at a final concentration of 50 μM apo-Mb to 5 μM holo-protein. The receptor has higher affinity for hemin as compared to Hb or Hb0.1. (b) Plots of the observed rate constants, $k_{\rm fast}$ (dark gray circles) and $k_{\rm slow}$ (light gray circles), versus the ratio of [α-IsdH] to [Hb0.1]. The concentration of Hb0.1 was held constant at 5 μM. The observed values were obtained in experiments similar to those described in the legend in Fig. 3. For $k_{\rm fast}$, fits to the data using Eqn. 1 are shown.

Figure 6. Temperature dependence of hemin transfer. (a) Representative normalized stopped-flow time courses as function of ΔA_{405} . They were obtained by mixing 5 μM Hb0.1 with 200 μM α-IsdH. Spectral traces were normalized using the following equation: $y = (y_t - y_0) / (y_t + y_0)$. (b) A plot of $\ln(k_{\text{fast}})$ /T) versus 1/T is shown. The observed k_{fast} values were obtained in experiments similar to those described in the legend in Fig. 3. The correlation factor, \mathbb{R}^2 , is indicated on the plot.

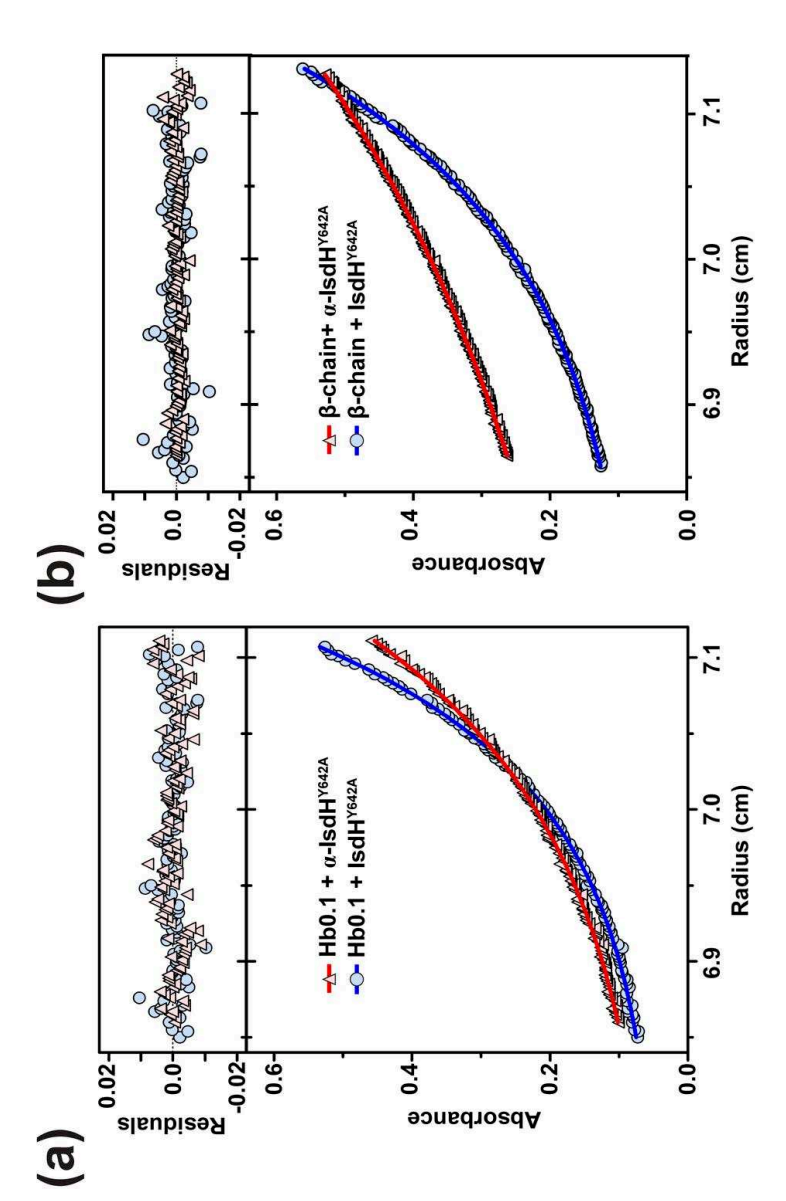
Figure 7. IsdH used two distinct interfaces to promote hemin transfer. (a) Representative ITC data for the titration of 200 μM α-IsdH^{Y642A} into 30 μM HbCO (heme/globin-chain basis). Injections were made at 180 s intervals at 25°C. (b) Representative ITC data for the titration of 300 μM α-IsdH^{N2} into 30 μM HbCO. (c) Representative ITC data for the titration of 850 μM α-IsdH^{LN3-Y642A} into 30 μM HbCO. The top panels show the time course of the titration (black) and baseline (red). The bottom panels show the integrated isotherms. ORIGIN software was used to fit the data to a single-site binding model to derive thermodynamic parameters. Receptors containing the N3 domain have a Tyr642Ala mutation that prevents hemin binding. (d) NMR titration data showing the effects of Hb binding on ¹⁵N-lableled polypeptides that contain only the N3 domain (IsdH^{N3-Y642A}, left) or the linker and N3 domains (IsdH^{LN3-Y642A}, right). The receptors contain a Tyr642Ala mutation that prevents hemin binding. ¹H-¹⁵N HSQC spectra of the proteins in the absence (top) or presence (bottom) of a 10-fold excess of HbCO tetramer are shown. Significant peak broadening is only observed when Hb is added to IsdH^{LN3-Y642A}, indicating that linker and N3 domains bind Hb, whereas the N3 domain in isolation does not bind to Hb.

Figure 8. Results of molecular dynamics simulations. (a) The hemoglobin dimer (gold) bound to hemin molecules (grey) and an IsdH^{N2N3} molecule (green and blue) was simulated, along with a system lacking IsdH^{N2N3} (not shown). (b) Radial distribution functions of solvent hydrogen (solid lines) and oxygen (dotted lines) atoms show that in the receptor bound system, solvent molecules are more frequently found at closer locations to the Nε-Fe bond then in the receptor free system. Analysis of simulations by a Grid Inhomogeneous Solvation Theory (GIST) analysis show that in IsdH^{N2N3} free systems (c&d) the number of hydration sites (cyan) surrounding the hemin group is limited, however, in the IsdH^{N2N3} bound systems (e&f) significantly more hydration sites are identified around the Nε-Fe bond.

Figure 9. Model of the hemin extraction mechanism. Proposed hemin transfer reaction coordinate diagram. The IsdH^{N2N3} receptor recognizes Hb via two energetically distinct interfaces (N2-Hb and LN3-Hb interfaces). Top, schematic showing the steps in hemin transfer. Bottom, relative free energies of the intermediates. Free energies calculated from this study are labeled along reaction coordinate diagram. Breakage of the axial Fe-Nɛ bond is presumably rate limiting (step #3). The following color scheme was used: N2, green; Linker-N3, blue; Hb a-subunit, gold.









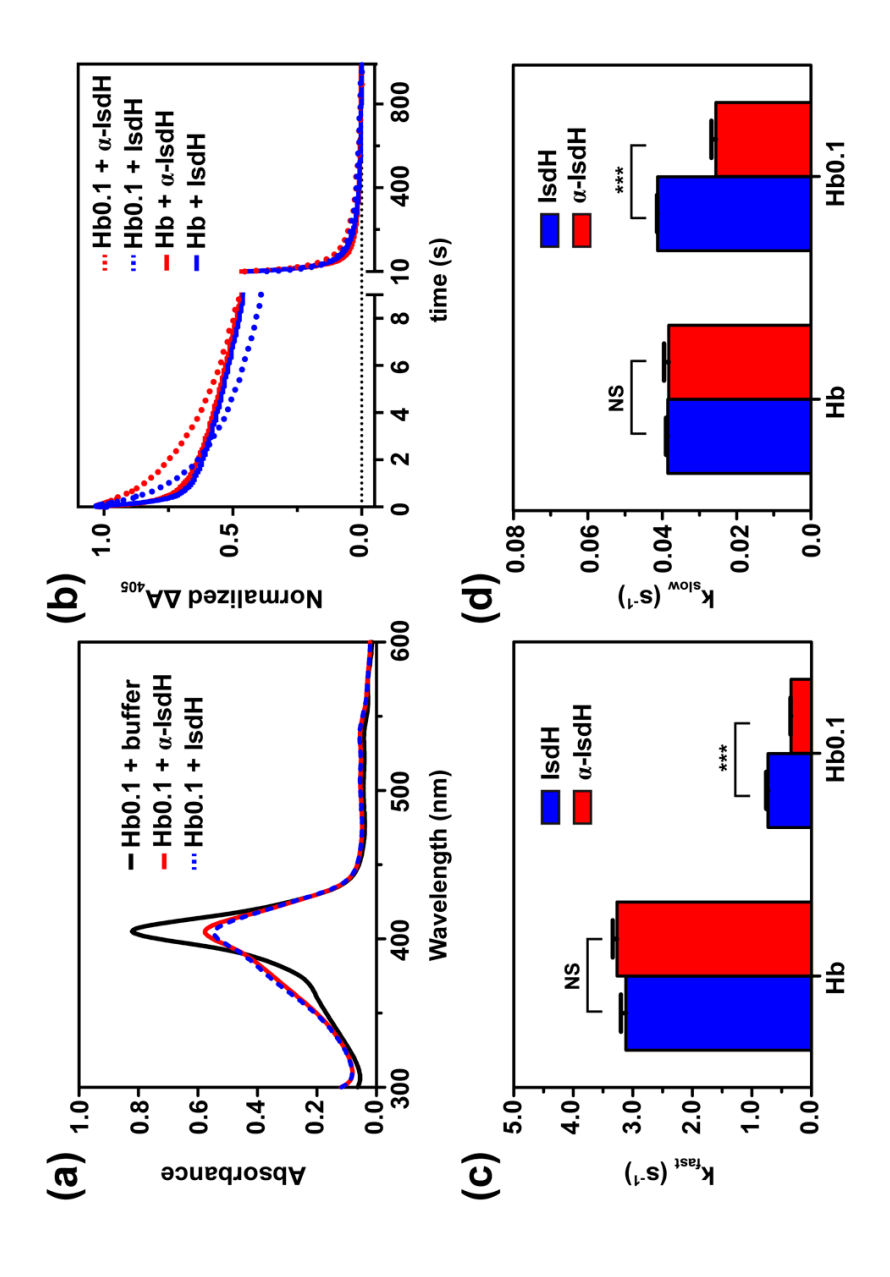
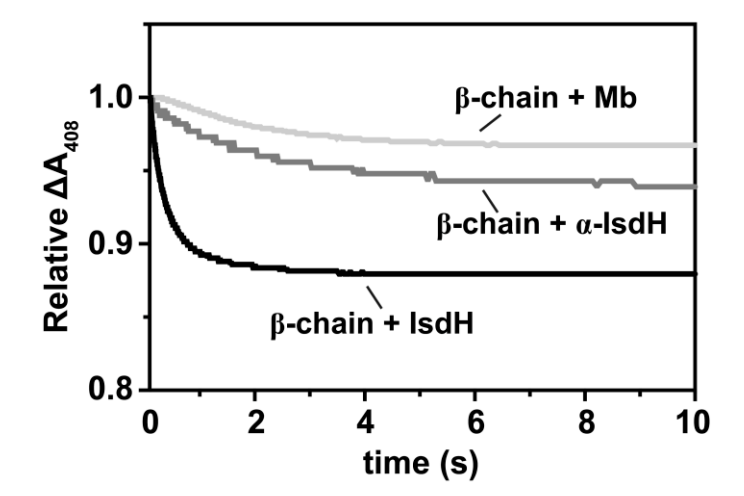


Figure 3

Figure 4





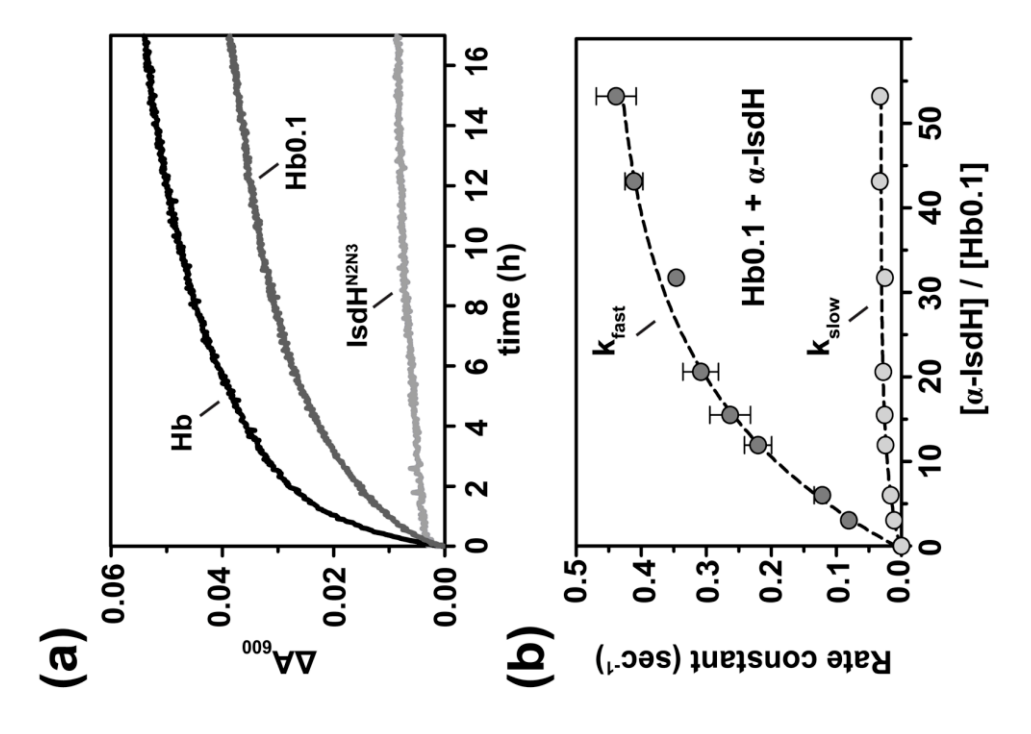


Figure 6

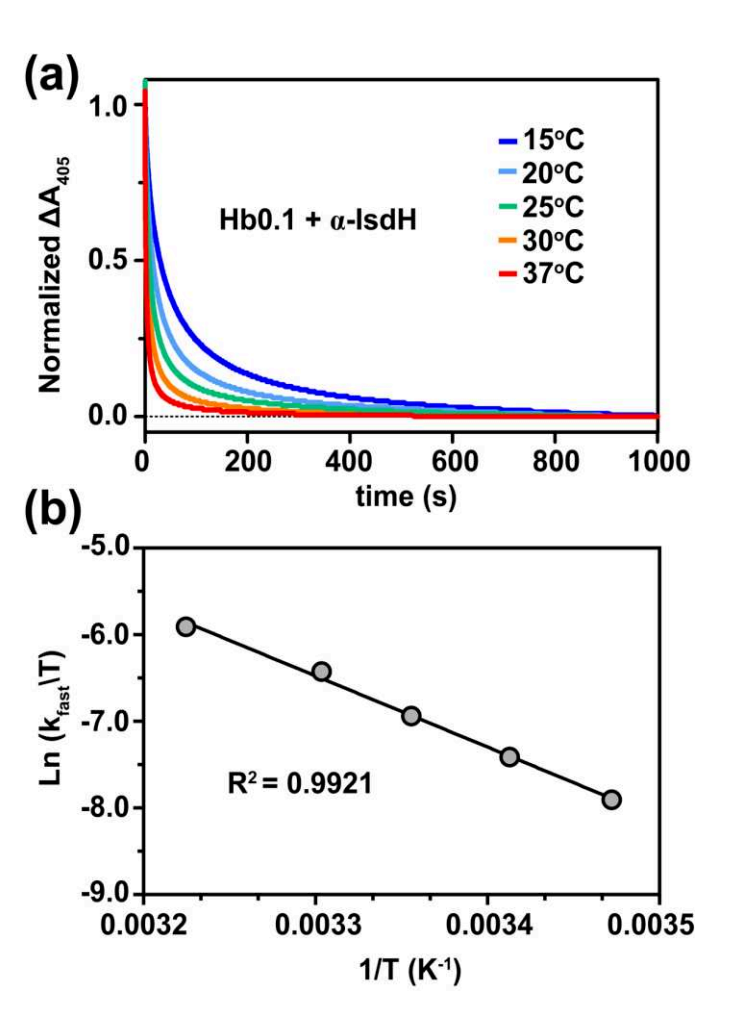
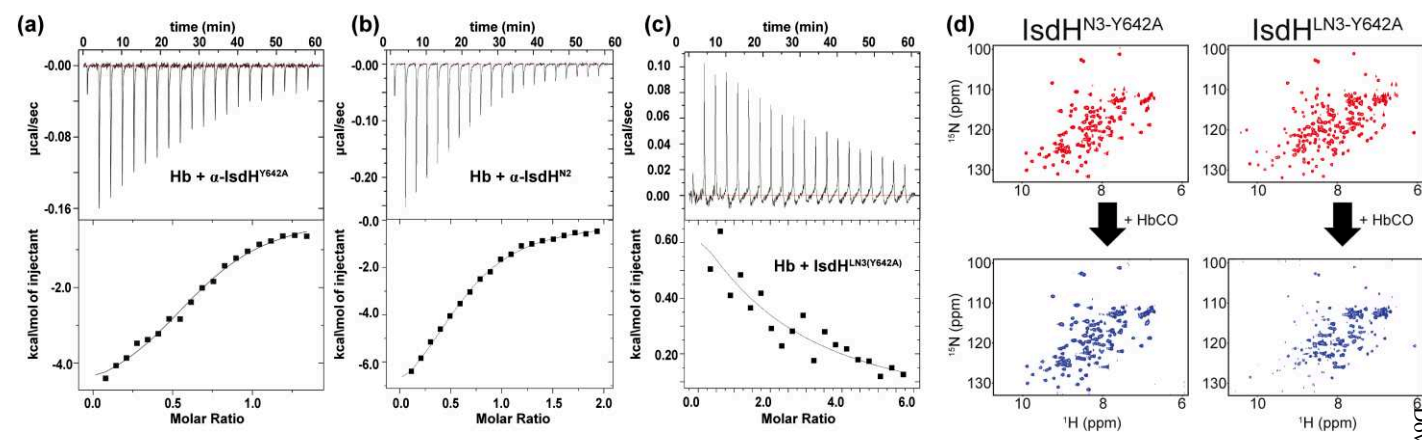


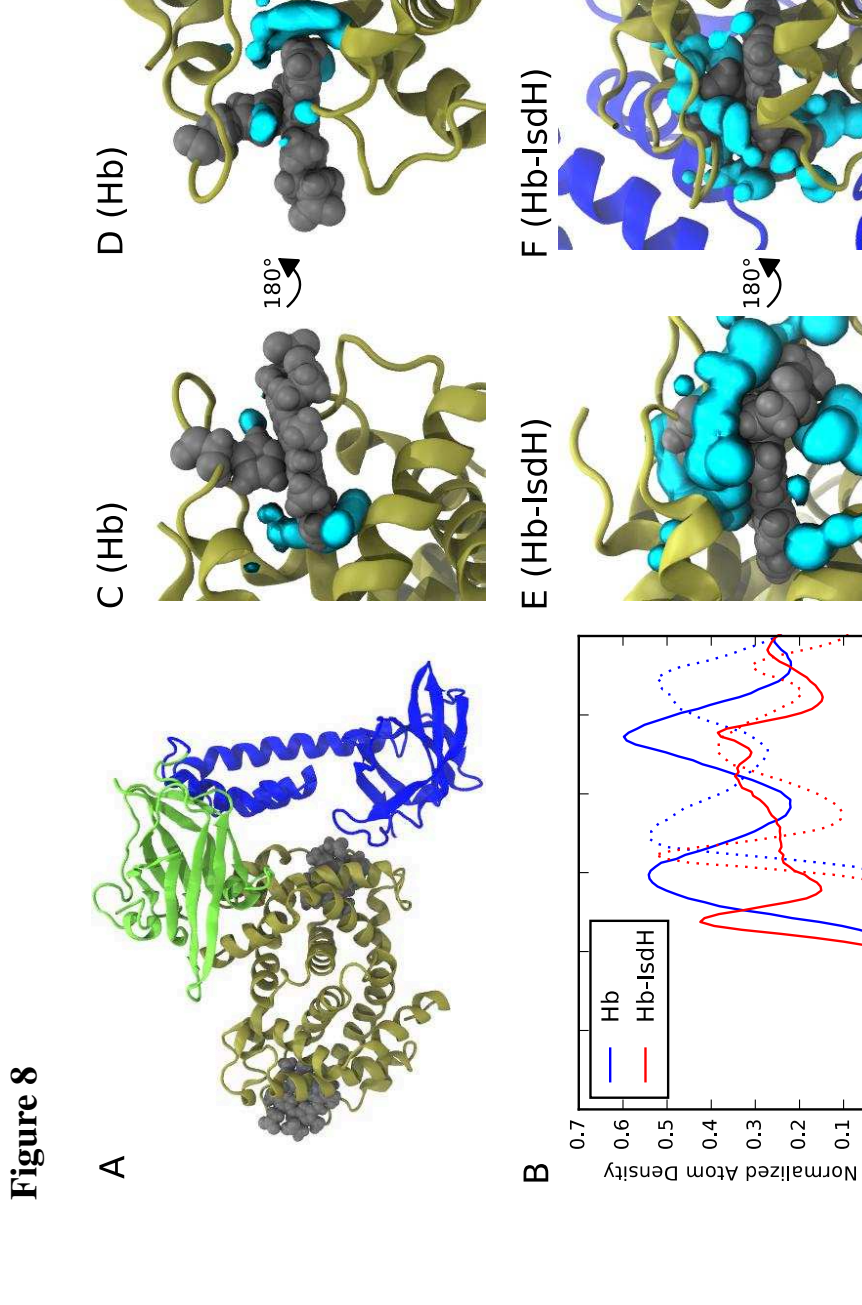
Figure 7



Distance From $N_{\rm e}\text{-Fe}$ Bond (Å)

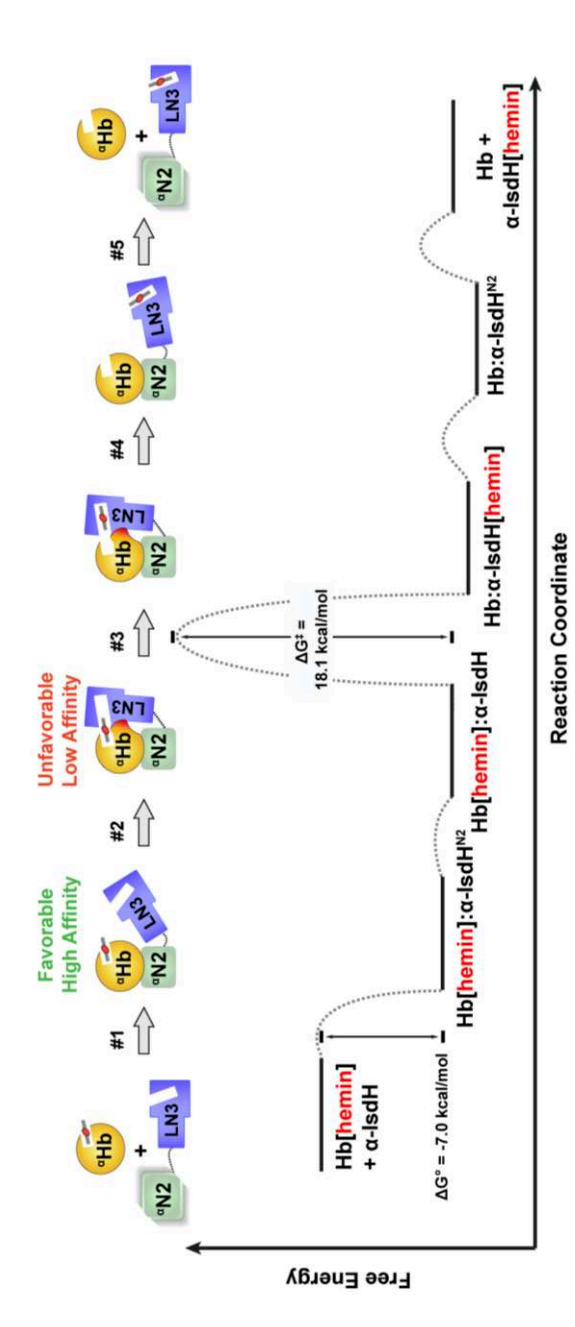
180

0.3 0.2



36





Energetics Underlying Hemin Extraction from Human Hemoglobin by Staphylococcus aureus

Megan Sjodt, Ramsay Macdonald, Joanna D. Marshall, Joseph Clayton, John S. Olson, Martin L. Phillips, David A. Gell, Jeff Wereszczynski and Robert T. Clubb

J. Biol. Chem. published online March 14, 2018

Access the most updated version of this article at doi: 10.1074/jbc.RA117.000803

Alerts:

- When this article is citedWhen a correction for this article is posted

Click here to choose from all of JBC's e-mail alerts